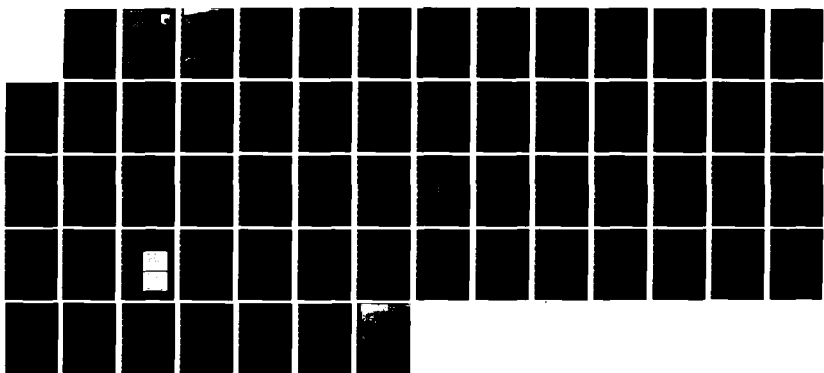
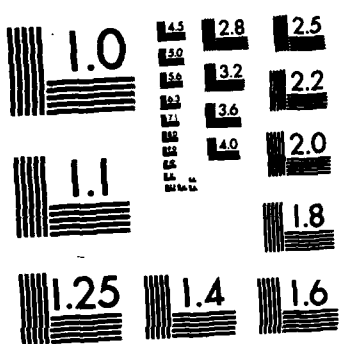


FD-A134 486 PULSE WIDTH MODULATED DC LINK CONVERTER DEVELOPMENT(U) 1/1  
GENERAL ELECTRIC CO BINGHAMTON NY ARMAMENT AND  
ELECTRICAL SYSTEMS DEPT C D HARBOUR JUN 83 AES-14018  
UNCLASSIFIED AFWAL-TR-83-2046 F33615-81-C-2061 F/G 10/2 NL





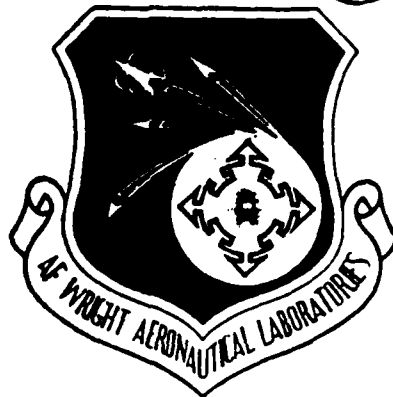
MICROCOPY RESOLUTION TEST CHART  
NATIONAL BUREAU OF STANDARDS-1963-A

AB-AI 34486

(12)

AFWAL-TR-83-2046

**PULSE WIDTH MODULATED  
DC LINK CONVERTER  
DEVELOPMENT**



GENERAL ELECTRIC COMPANY  
P.O. BOX 5000  
BINGHAMTON, NEW YORK 13902

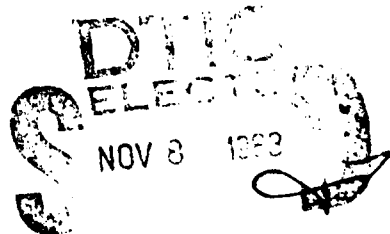
JUNE 1983

**FINAL REPORT FOR PERIOD SEPTEMBER 1981 — SEPTEMBER 1982**

FILE COPY  
DRAFT

APPROVED FOR PUBLIC RELEASE; DISTRIBUTION UNLIMITED

AERO PROPULSION LABORATORY  
AIR FORCE WRIGHT AERONAUTICAL LABORATORIES  
AIR FORCE SYSTEMS COMMAND  
WRIGHT-PATTERSON AIR FORCE BASE, OHIO 45433



83 11 07 066

NOTICE

When Government drawings, specifications or other data are used for any purpose other than in connection with a definitely related Government procurement operation, the United States Government thereby incurs no responsibility nor any obligation whatsoever; and the fact that the government may have formulated, furnished, or in any way supplied the said drawings, specifications or other data, is not to be regarded by implication or otherwise as in any manner licensing the holder or any other person or corporation or conveying any rights or permission to manufacture, use, or sell any patented invention that may in any way be related thereto.

This report has been reviewed by the Office of Public Affairs (ASD/PA) and is releasable to the National Technical Information Service (NTIS). At NTIS, it will be available to the general public, including foreign nations.

This technical report has been reviewed and is approved for publication.

William Berger

---

Mr. W. Berger  
Acting Technical Area Manager  
Power Systems Branch

David Schorr

---

Major David Schorr  
Chief  
Power Systems Branch

FOR THE COMMANDER

James D. Reams

James D. Reams  
Chief, Aerospace Power Division  
Aero Propulsion Laboratory

Copies of this report should not be returned unless return is required by security consideration, contractual obligation, or notice on a specific document.

Unclassified

**SECURITY CLASSIFICATION OF THIS PAGE (When Data Entered)**

| REPORT DOCUMENTATION PAGE  |  | READ INSTRUCTIONS<br>BEFORE COMPLETING FORM   |
|--|--|---|
| 1. REPORT NUMBER<br><b>AFWAL-TR-83-2046</b>  | 2. GOVT ACCESSION NO.<br><b>AD-A134486</b> | 3. RECIPIENT'S CATALOG NUMBER   |
| 4. TITLE (and Subtitle)<br><br><b>PULSE WIDTH MODULATED DC LINK<br/>CONVERTER DEVELOPMENT</b>  |  | 5. TYPE OF REPORT & PERIOD COVERED<br><br>Final Report for Period<br>Sept 1981 - Sept 1982                                    |
| 7. AUTHOR(s)<br><br><b>C.D. Harbourt</b>   |  | 6. PERFORMING ORG. REPORT NUMBER<br><br><b>AES-14018</b>  |
| 9. PERFORMING ORGANIZATION NAME AND ADDRESS<br><br><b>General Electric Company<br/>P.O. Box 5000<br/>Binghamton, NY 13902</b>  |  | 10. PROGRAM ELEMENT, PROJECT, TASK AREA & WORK UNIT NUMBERS<br><br><b>PE 62203F, Project 3145<br/>Task 31429, WU 31452967</b> |
| 11. CONTROLLING OFFICE NAME AND ADDRESS<br><br><b>Aero Propulsion Laboratory (AFWAL/POO)<br/>Air Force Wright Aeronautical Lab, AFSC<br/>Wright Patterson AFB, Ohio 45433</b>  |  | 12. REPORT DATE<br><br><b>June 1983</b>   |
| 14. MONITORING AGENCY NAME & ADDRESS (if different from Controlling Office)  |  | 13. NUMBER OF PAGES<br><br><b>61</b>  |
|  |  | 15. SECURITY CLASS. (of this report)<br><br><b>Unclassified</b>   |
|  |  | 15a. DECLASSIFICATION/DOWNGRADING SCHEDULE  |
| 16. DISTRIBUTION STATEMENT (of this Report)<br><br><b>Approved for public release, unlimited distribution</b>  |  |   |
| 17. DISTRIBUTION STATEMENT (of the abstract entered in Block 20, if different from Report)   |  |   |
| 18. SUPPLEMENTARY NOTES  |  |   |
| 19. KEY WORDS (Continue on reverse side if necessary and identify by block number)<br><br><b>Pulse Width Modulation<br/>DC Link<br/>VSCF (Variable Speed Constant Frequency)</b>   |  |   |
| 20. ABSTRACT (Continue on reverse side if necessary and identify by block number)<br><br><b>Further development of power transistor and power Darlington current carrying and voltage blocking capabilities led to the application of new General Electric devices in a 40 KVA Pulse Width Modulated DC Link VSCF system. The results indicate that the power Darlington devices selected exhibit large losses at the switching frequencies studied. Because of these losses, the devices (in their present status) are considered unacceptable for use in a DC VSCF system.</b> |  |   |

## FOREWORD

This final report was submitted by the Armament and Electrical Systems Department of the General Electric Company under contract F33615-81-C-2061. This effort was sponsored by the Air Force Wright Aeronautical Laboratory, Air Force Systems Command with Dr. W.U. Borger, AFWAL-POOS-2 as Project Engineer. Craig H. Jennings, General Electric Company, was Program Manager and responsible for the overall effort.

This report covers work during the period September 1981 to September 1982. The final report was submitted to AFWAL in February 1983.

The author gratefully acknowledges the contributions made by D. Lafuze, J. Butler, W.J. Thomas, M.R. Shah, E.U.A. Siddiqui, J. Summerford, T. Wilson and A. Foss of General Electric Armament and Electrical Systems Department.

|               |                |
|---------------|----------------|
| Accession For | NTIS GRANT     |
| DATA TAB      | UNCLASSIFIED   |
| JULY 1983     | IDENTIFICATION |
| DATA TAB      | REF ID: A-1    |
| DATA TAB      | A-1            |



## CONTENTS

| <u>Section</u> |  | <u>Page</u> |
|----------------|--|-------------|
| I              | INTRODUCTION.....                                | 1           |
|                | 1.0 Objective.....                               | 1           |
|                | 2.0 Scope.....                                   | 1           |
|                | 3.0 Background.....                              | 2           |
| II             | CONCLUSIONS AND RECOMMENDATIONS.....             | 3           |
|                | 1.0 Conclusions.....                             | 3           |
|                | 2.0 Recommendations.....                         | 3           |
| III            | ORIGINAL CIRCUIT DEVELOPMENT.....                | 4           |
|                | 1.0 Design.....                                  | 4           |
|                | 2.0 Design Considerations.....                   | 8           |
| IV             | INTERPHASE TRANSFORMER INVERTER DESCRIPTION..... | 17          |
| V              | GENERATOR DESIGN.....                            | 27          |

| <u>Appendixes</u> |   | <u>Page</u> |
|-------------------|---|-------------|
| A                 | Original Description of CMOS Logic..... | 33          |
| B                 | Fourier Analysis of PWM Waveform.....   | 45          |
| C                 | Darlington Parallelizing Study.....     | 50          |

## LIST OF ILLUSTRATIONS

| <u>Figure</u> |   | <u>Page</u> |
|---------------|---|-------------|
| 1             | Original Power Circuit.....                             | 5           |
| 2             | Triangular Wave - Reference Wave Comparison.....        | 6           |
| 3             | Base Drive Timing.....                                  | 7           |
| 4             | Proportional Base Drive Circuit.....                    | 10          |
| 5             | New Base Drive.....                                     | 11          |
| 6             | Isolated 400 Hz Base Drive.....                         | 12          |
| 7             | Voltage Spike Problem.....                              | 13          |
| 8             | Positive-Negative Zero Crossing.....                    | 14          |
| 9             | 9600/19200 Hz Switching Sequence.....                   | 16          |
| 10            | IPT Inverter-Power Circuit.....                         | 18          |
| 11            | IPT Inverter-Switching Sequence.....                    | 20          |
| 12            | IPT Inverter-Current and Voltage Positive.....          | 22          |
| 13            | IPT Inverter-Current Negative, Voltage<br>Positive..... | 22          |
| 14            | Ripple Volt-Sec vs Volts.....                           | 24          |
| 15            | Individual Inductors vs IPT.....                        | 25          |
| 16            | Generator Layout.....                                   | 28          |
| 17            | Generator Adapter.....                                  | 30          |
| 18            | Generator Oil Flow Schematic.....                       | 31          |
| 19            | P-18 Stator Frame .....                                 | 32          |

| <u>Appendices</u> |   | <u>Page</u> |
|-------------------|---|-------------|
| A-1               | PWM CMOS Logic - Single Phase Output.....   | 35          |
| A-2               | Divide by Three Counter.....  | 37          |
| A-3               | PWM Voltage Comparators.....  | 38          |
| A-4               | Voltage Spike Blanking Circuit.....   | 41          |
| A-5               | Reference Wave Filter and DC Feedback.....  | 42          |
| A-6               | Complement Circuit.....   | 43          |
| A-7               | Complement Circuit Timing Diagram.....  | 44          |
| B-1               | PWM Waveform.....   | 47          |
| C-1               | Current Sharing and Matching Definition.....  | 52          |
| C-2               | Switching/Paralleling Circuit.....  | 53          |
| C-3               | Base Drive Used by Solid State Applications<br>Organizations, General Electric Company..... | 54          |

## Section I INTRODUCTION

### 1.0 OBJECTIVE

This program was an exploratory development effort to design, develop and test a 400 hz variable speed constant frequency (VSCF) type power system which employs a pulse width modulated (PWM) converter operating in conjunction with a variable voltage/frequency permanent magnet generator (PMG)\*. The program objective was to demonstrate an advanced generating system concept which would yield performance, efficiency, volume, weight and cost advantages over state-of-the art VSCF systems. The converter/generator was to have been tested in a prototype system with the following general characteristics: 1) 40 KVA system rating, 115V, 30, 400 Hz, 2) Base speed as required, and 3) Minimum speed range 2:1.

### 2.0 SCOPE

This effort included the following tasks: 1) Design of a prototype permanent magnet generator, 2) Design of a "brassboard" converter, 3) Fabrication of the generator and the converter, 4) Generator and converter testing, 5) System testing and 6) Reporting. The program was to be accomplished in the distinct phases

---

\*The term pulse width modulated (PWM) will be used throughout this report as nomenclature for DC to AC conversion devices which create AC from DC via high speed solid state switching devices. A typical example of waveform construction via this technique is shown in Figure 2.

identified below. The time periods in parentheses were Air Force estimates of the times required to accomplish each phase.

Phase I - Design (6 months)

Phase II - Hardware Fabrication (11 months)

Phase III - Tests (7 months)

The following tasks were completed as a part of this effort:

- a) Design of a prototype permanent magnet generator
- b) Design of two different breadboard converters
  - 1) Bridge Inverter (Original Design)
  - 2) Interphase Transformer Inverter
- c) Limited breadboard converter testing
- d) Reporting.

### 3.0 BACKGROUND

There are three alternative technologies available today for the manufacturer who wishes to design an aircraft electrical power system. These are the cycloconverter, as is used in the F-18 and A4 VSCF systems, the constant speed drive-synchronous generator combination, and the DC link VSCF approach, used on the AV-8B and the F-5G.

Recent developments in the field of high power Darlington pair configured transistors have increased both current carrying capability and blocking voltage to the point that high power (40 KVA) pulse width modulated inverters are possible. These inverters, when used with a rectifying SCR bridge, should provide a DC link system competitive in size, weight, and electrical performance with cycloconverter and constant speed drive systems.

## Section II

### CONCLUSIONS AND RECOMMENDATIONS

#### **1.0 CONCLUSIONS**

The work done by the General Electric Company during the project has resulted in the conclusion that a 40 KVA pulse width modulated DC Link VSCF using state-of-the-art Darlington transistors is not viable at this time. The devices chosen for this application had much lower base drive current requirements than discrete power transistors of equivalent rating and were lower in cost than other comparable Darlington pairs. Despite these advantages, high power Darlington transistor technology is not sufficiently advanced for a DC Link system to possess size, weight and efficiency advantages over other comparable VSCF technologies.

#### **2.0 RECOMMENDATIONS**

This program did not produce a 40 KVA PWM VSCF which could meet all the required specifications, because of device inadequacies. A concerted effort should be made to further develop the transistor technology to the point where it becomes technically viable in the PWM application.

## Section III ORIGINAL CIRCUIT DEVELOPMENT

### 1.0 DESIGN

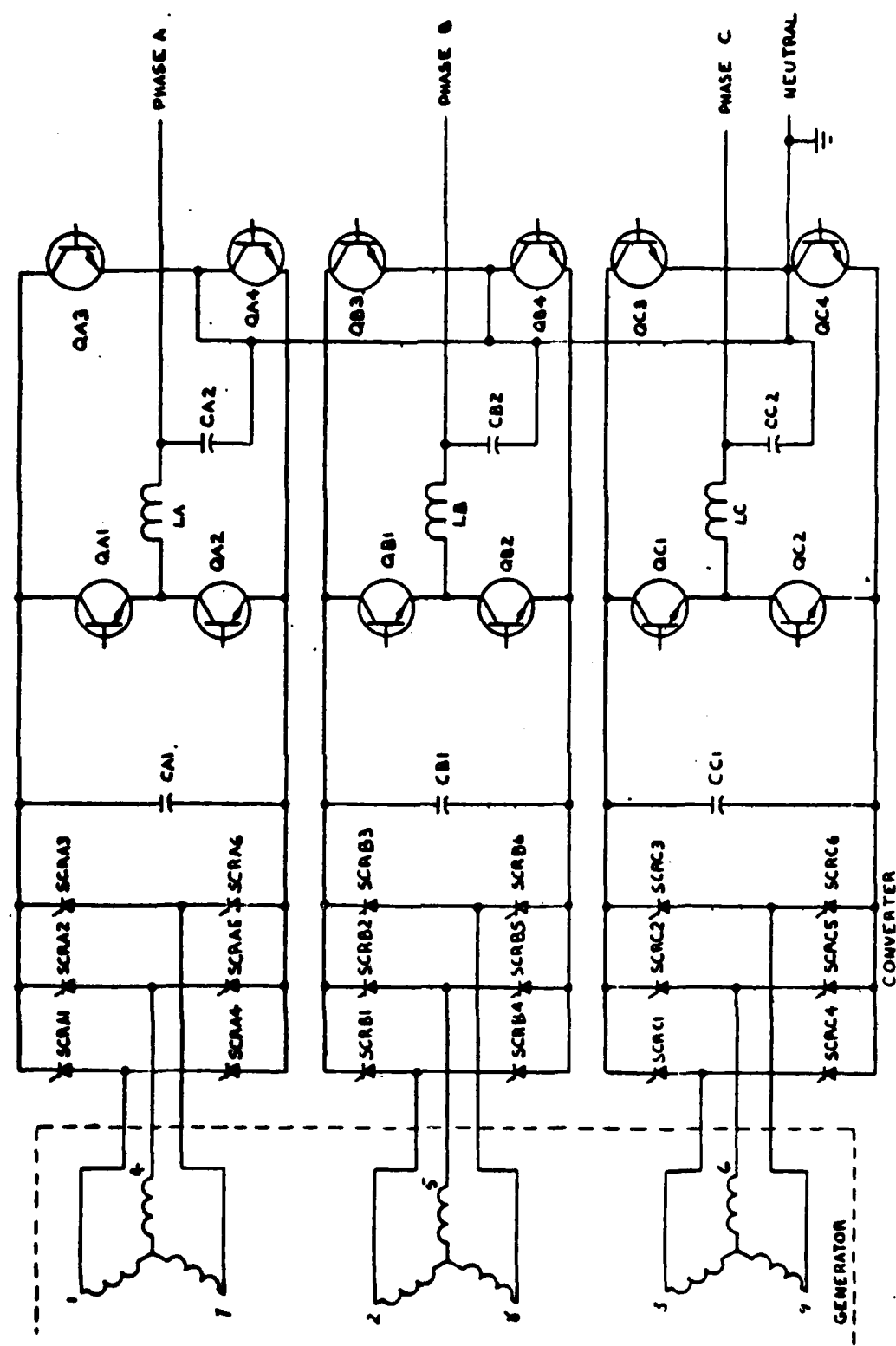
The original concept for the PWM converter design was to use a 9 phase PMG and 3 three phase SCR bridges to generate 3 separate DC links of approximately 200 volts DC each (Figure 1). These DC voltages would then be converted to 3 $\phi$  115/208 volt AC using three H bridge inverters with output filters used to eliminate output harmonics. These bridges would use 500 volt, 200 amp ZJ504 General Electric Darlington transistors to enable the output voltage of the inverters to be pulse width modulated.

The algorithm chosen to accomplish this was to compare a variable amplitude sinusoidal reference wave with a fixed amplitude high frequency triangular carrier wave (Figure 2). The frequency of this carrier wave determined the necessary filter size. The original concept set this frequency at 4800 hz with a 400 hz sinusoidal reference.

The output of the PWM logic was then fed to a proportional base drive to drive two of the Darlington transistors (located in the upper two legs of the inverter bridge) at a 4800 hz rate. The other two Darlintons (in the lower two legs of the bridge) were driven at a 400 hz rate by a 400 hz square wave, generated by detecting the zero crossings of the reference wave. So, two of the legs of the inverter would conduct to produce positive or negative voltage across the load and filter. The conducting legs were determined by which half cycle of output voltage was being generated (Figure 3).

To test this concept a prototype breadboard was built using General Electric D67DE7 700 volt, 100 Amp Darlington pair transistors. The control logic was 2 circuit cards with standard 4000 series CMOS logic.

Figure 1. Original Power Circuit



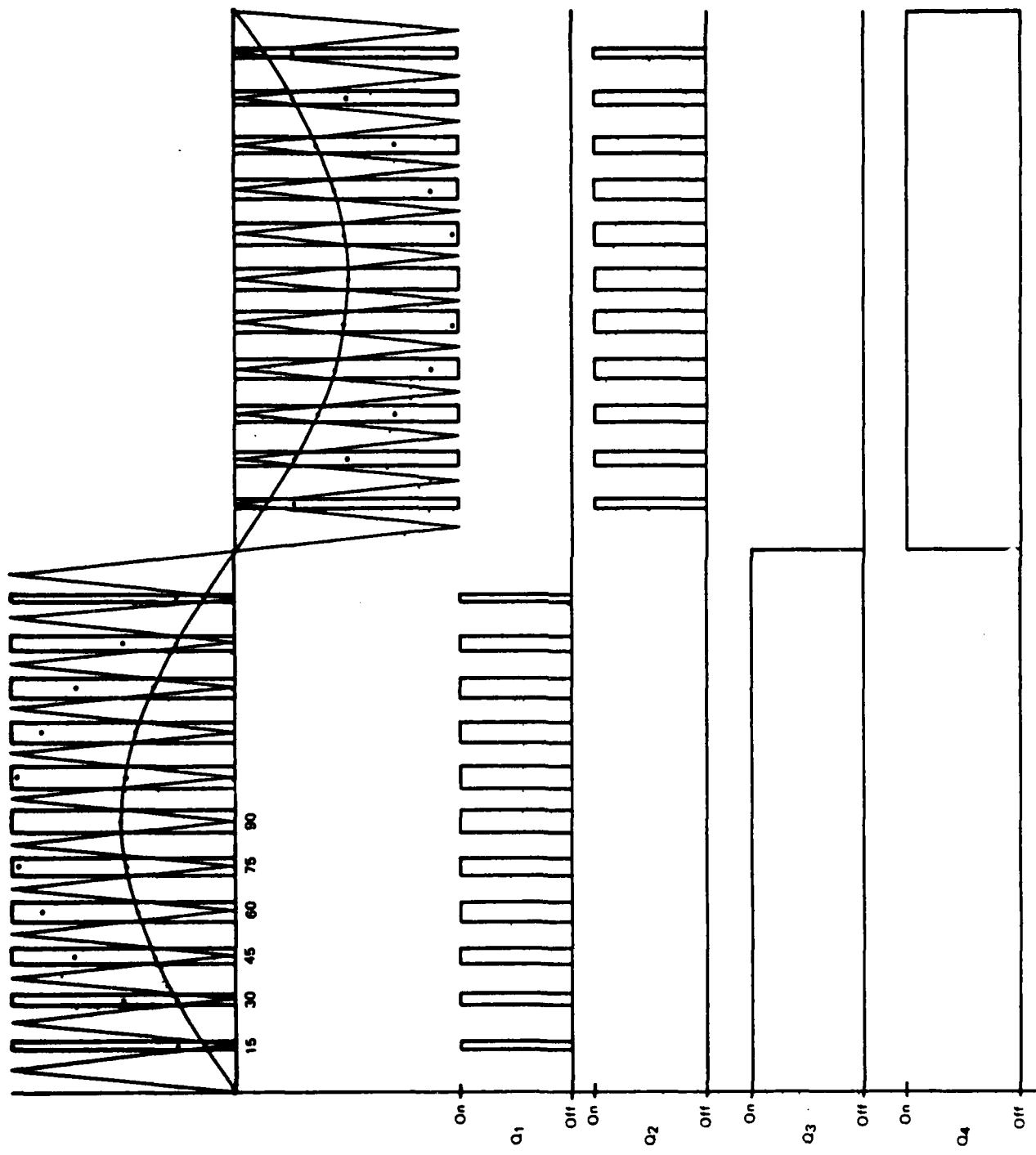


Figure 2. Triangular Wave-Reference Wave Comparison

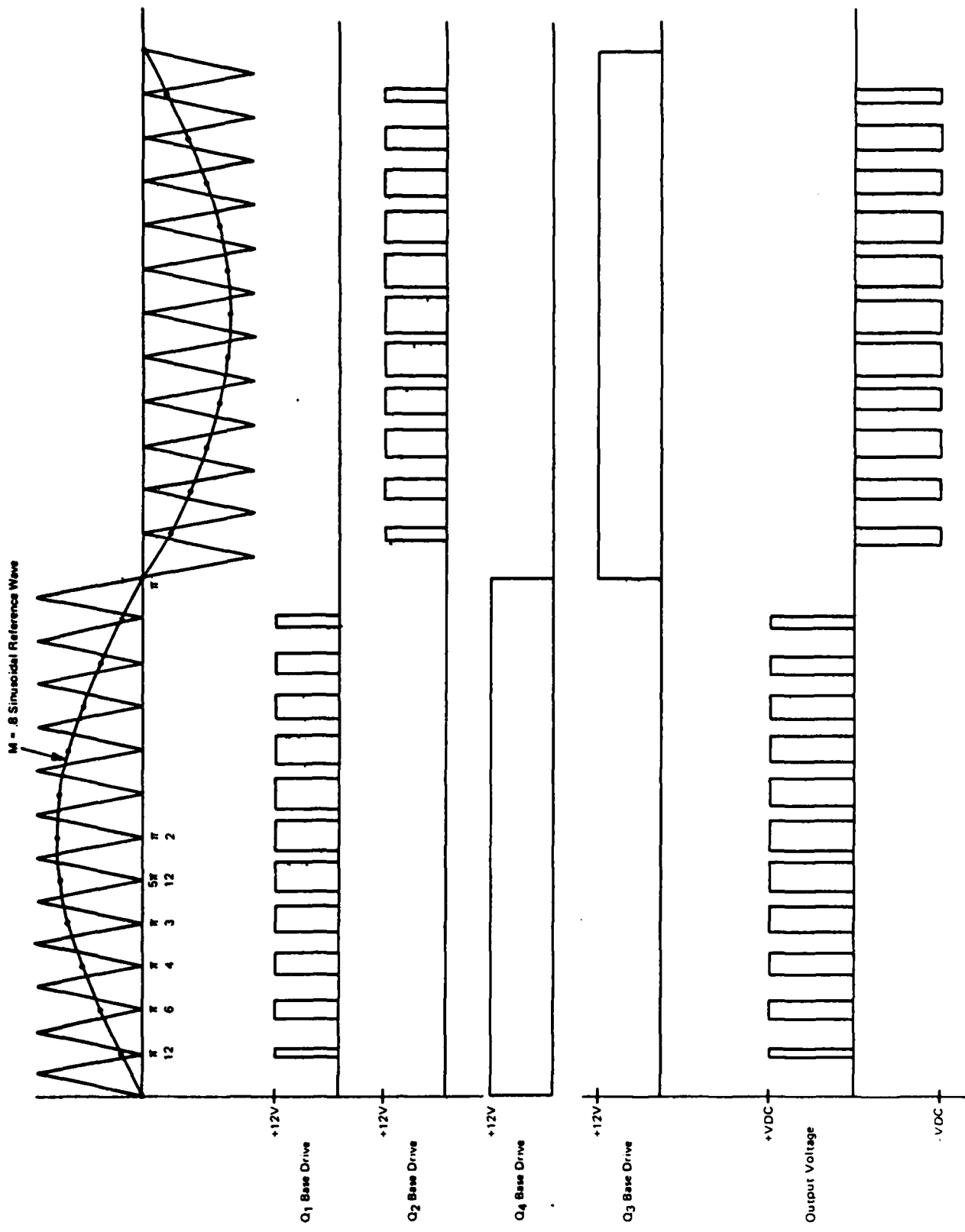


Figure 3. Base Drive Timing

## **2.0 DESIGN CONSIDERATIONS**

There were four areas in which changes from the original circuit were found to be necessary after extensive breadboard testing. These were as follows:

- 1) Output Filter Size
- 2) Proportional Base Drive Saturation
- 3) Location of Signal Ground
- 4) Undesirable Voltage Spikes at Zero Crossings.

This testing process exposed these areas as places where the design could be optimized and trade-offs made to improve the system performance.

The first consideration was that the output filter was required to be too large ( $212\mu\text{h}$ ,  $120\mu\text{f}$ , a corner frequency of 998 Hz) to reduce the output harmonics of the bridge voltage to acceptable levels. The energy in the output harmonics was concentrated around 4800 Hz, the frequency of the triangular carrier wave mentioned earlier. The effect is characteristic of PWM inverters which are modulated by triangular carriers and has been mentioned in several papers, Reference 1 being one such paper.

This problem of low frequency output harmonics and output filter size made it necessary to change the fundamental carrier wave frequency from 4800 to 9600 Hz. This change enabled the output filter inductor to change from  $212\mu\text{h}$  to  $121\mu\text{h}$ , yielding a break frequency of 1320.8 Hz. This change was possible because the new carrier wave frequency concentrated the bridge voltage harmonic energy around 9600 Hz, rather than 4800 Hz.

The second consideration was that the magnetics in the proportional base drive circuit (Figure 4) saturated in the middle of the output voltage waveform as the DC link voltage was increased, causing additional distortion in the output voltage. In addition, the base drive requirement of Darlington connected transistor pairs are not as severe as originally thought, so the proportional base drive was found not to be necessary. A new base drive circuit using MOSFET transistors (Figure 5) was used to replace the original proportional base drive circuit.

Using MOSFET devices reduced the parts count of the base drive by a factor of 4 to 1. In addition, it reduces the delay time between logic level signals and the output voltage of the inverter bridge. An additional consideration was that the current in each Darlington pair was no longer coupled to the base drive, so the magnetics in the new base drive did not saturate.

The third consideration was the location of signal ground. Originally, signal ground was located at the negative side of the DC supply, enabling the use of directly supplied base drives for the Darlington pairs switched at 400 Hz. However, it was more advantageous for feedback purposes to have signal ground at an emitter of one of the Darlington pairs whose base drive was pulse width modulated. This necessitated using an isolated drive for the Darlington pairs which were switched at 400 Hz (Figure 6).

The fourth consideration was undesirable voltage spikes at zero crossings of the reference wave. The reason for this was the switching between the two Darlington pairs at 400 Hz at the zero crossing points of the reference wave.

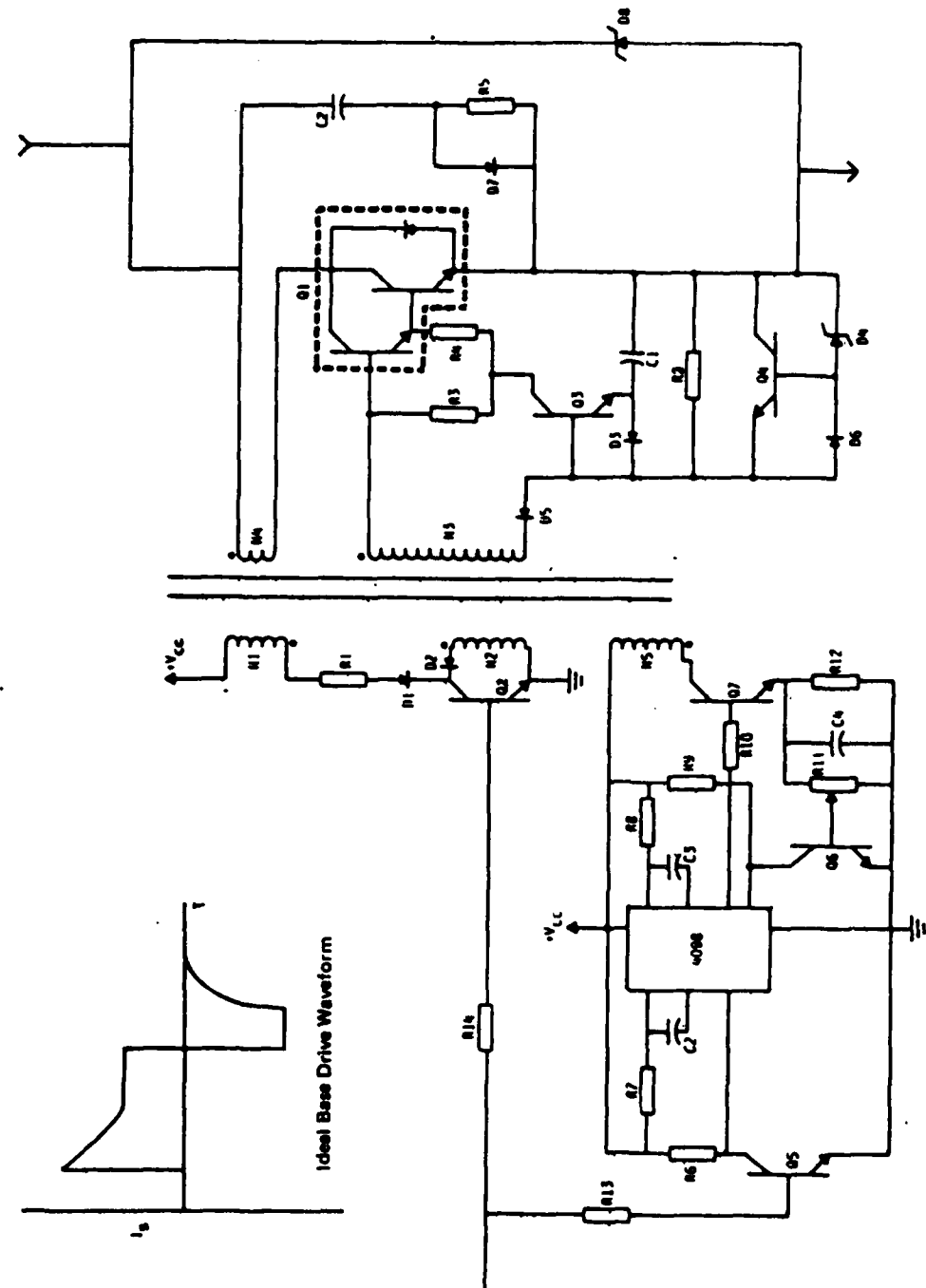
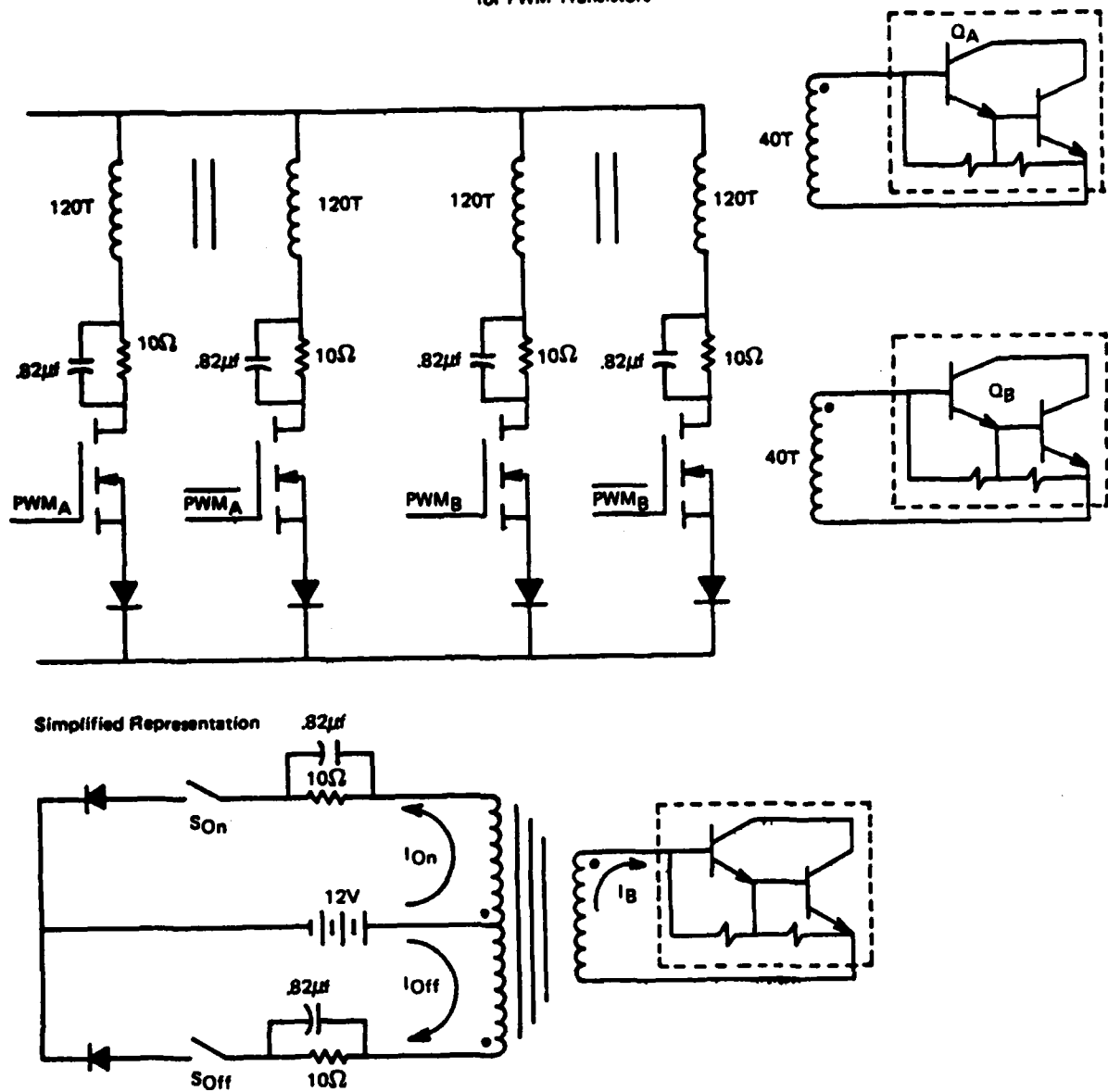


**Figure 4.** Proportional Base Drive Circuit

Alternative Base Drive  
for PWM Transistors



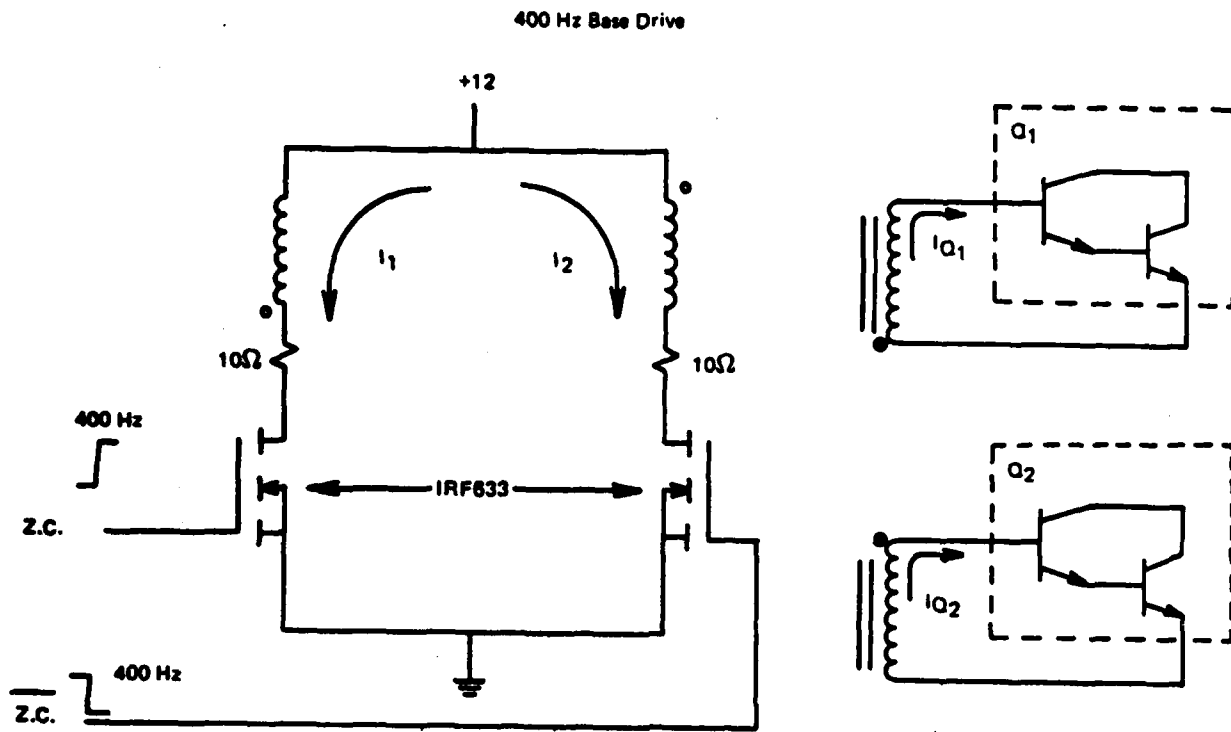
Produces waveform similar to ideal base drive waveform

Switching times below 1μs using MOSFET drives

Less complex (fewer parts) than proportional base drive

Proportional drive not necessary for Darlington transistor pairs (Darlingtons have low base current at rated current levels, unlike single BJT application).

Figure 5. New Base Drive



When the Zero Crossing (Z.C.) signal is +12 volts,  $I_1$  flows, inducing a current  $I_{Q_1}$  to flow, turning on Darlington pair  $Q_1$ . When the inverted zero crossing signal (Z.C.) is +12 volts,  $I_2$  flows, inducing  $I_{Q_2}$  to flow, turning on Darlington pair  $Q_2$ . Using the IRF633 MOSFET devices enables the circuit to have switching time delays within the specification of the D67DE 100 Amp GE Darlington. Using bipolar devices adds 2-4  $\mu$ s to the switching time delays.

**Figure 6.** Isolated 400 Hz Base Drive

If the current I in Figure 7 is nonzero when  $S_4$  switches off and  $S_3$  switches on, diodes  $D_3$  and  $D_2$  conduct until I is zero. This conduction made  $V_{BR} = -V_{DC}$  at a time when that condition was not desired, e.g., at the zero crossing of the 400 Hz reference wave.

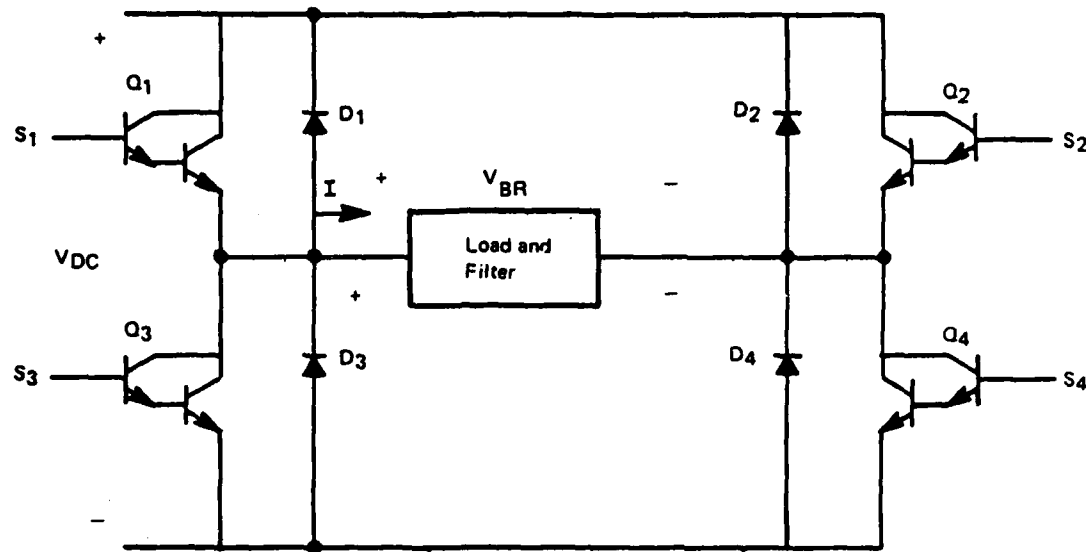
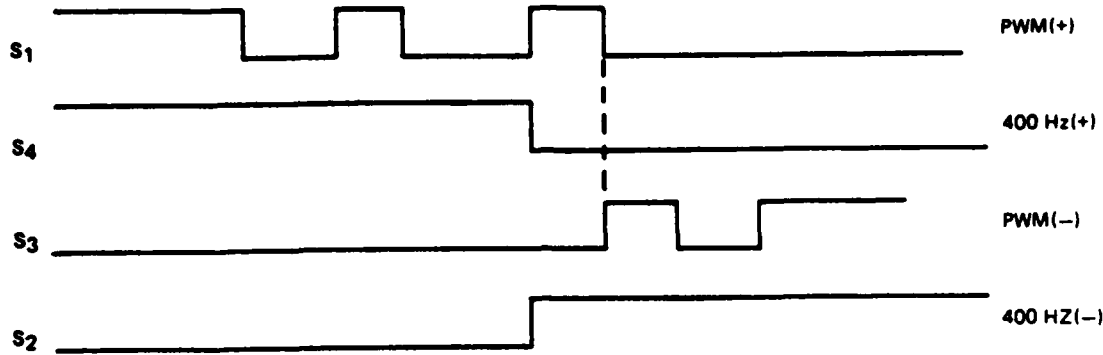


Figure 7. Voltage Spike Problem

This problem was resolved by reconfiguring the circuit so that both Darlington pairs switched at 400 Hz were on the ground side of the bridge, turning on  $Q_1$ , after the positive-negative zero crossing until  $S_3$  requires  $Q_3$  to turn on, and turning on  $Q_3$  after the negative-positive voltage zero crossing until  $S_1$  requires  $Q_1$  to turn on (See Figure 8).



**Figure 8. Positive-Negative Zero Crossing**

Referencing Figure 7, assume  $I_{pos}$  flows through  $Q_1$  and  $Q_4$  initially. During the times when  $Q_1$  is off, current flows through  $D_3$  and  $Q_4$ . At the zero crossing of the reference wave,  $Q_4$  turns off and  $Q_2$  turns on. However, if  $I_{pos}$  still flows in the same direction, it must flow through  $D_2$  and  $D_3$ . To prevent this from happening,  $Q_1$  is turned on again after the zero crossing. This provides a path for  $I_{pos}$  to flow (through  $Q_1$  and  $D_2$ ) which prevents  $V_{DC}$  from appearing across the load until  $Q_3$  turns on again. In this manner, this change eliminated the unwanted zero crossing voltage spike.

This consideration led to the idea of switching  $S_1$  and  $S_3$  in a complimentary fashion so that lagging current will always have a path to flow. To accomplish this,  $S_1$  and  $S_3$  were changed so that  $S_1 = \text{PWM (+)} + \overline{\text{PWM (-)}}$  and  $S_3 = \text{PWM (-)} + \overline{\text{PWM (+)}}$ . A  $5\mu\text{s}$  delay was introduced in the inverted PWM signals to prevent shorting of the DC voltage through  $Q_1$  and  $Q_3$ .

Appendix A contains a detailed description of how these signals were generated with CMOS logic.

At this point, the output filter inductor size was still not optimal, and the switching rate on the two PWM transistors ( $Q_1$  and  $Q_3$ ) could not be doubled again to 19,200 Hz without creating unacceptably high switching losses in the D67DE7 devices. So, a new switching algorithm was developed (originally for use in the IPT inverter discussed in Section IV) which was applied to the original circuit as well. This algorithm, shown in Figure 9, caused all four Darlington pairs to switch at 9600 Hz, while the output voltage switched at 19,200 Hz. This enabled the output inductor size to be reduced to 40  $\mu$ H as opposed to 121  $\mu$ H in the original circuit. A new control circuit and two more MOSFET base drives were built, but the algorithm was not tested in the original breadboard at full voltage before work was halted.

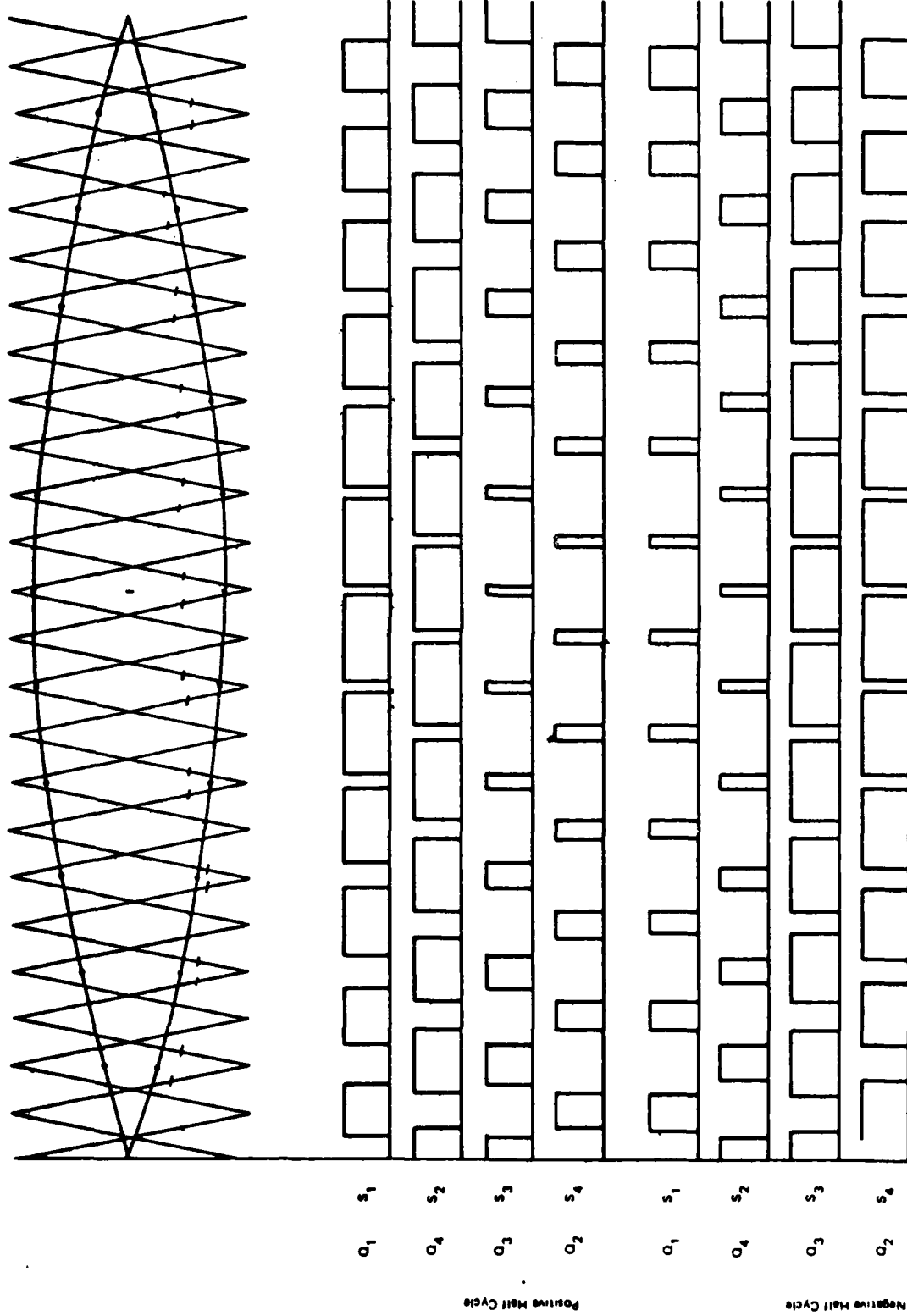


Figure 9. 9600/19200 Hz Switching Sequence

## Section IV

### INTERPHASE TRANSFORMER INVERTER DESCRIPTION

#### 1.0 DESIGN

The approach to DC link discussed in Section III was the version which was presented in the proposal. That approach, using 3 three phase rectifier bridges and 3 inverter bridges was not the most economical in terms of parts count. After much consideration, General Electric developed an approach which appeared attractive compared with both the bridge circuit General Electric had been pursuing and alternative approaches which require either a neutral forming transformer or a full output transformer. This new circuit uses the interphase transformer concept to provide the advantages of current sharing and reduced ripple that it has traditionally done for rectifier circuits.

Figure 10 shows the power circuit. The switches can be transistors, gate turn off devices or thyristors if commutation means are provided. The interphase transformer (IPT) is normally designed with a small air gap in its magnetic path to accommodate some DC current resulting from imperfect switching patterns. All or part of the separate filter inductance can be designed into the IPT.

In Figure 10, a center tapped DC supply ( $\pm 180V$ ) is shown supplying three IPT inverters. In comparing this arrangement with the circuit shown in Figure 1, two differences are noted.

- 1) One third fewer parts than the three 3 $\phi$  rectifier bridges (12 SCRs vs 18).

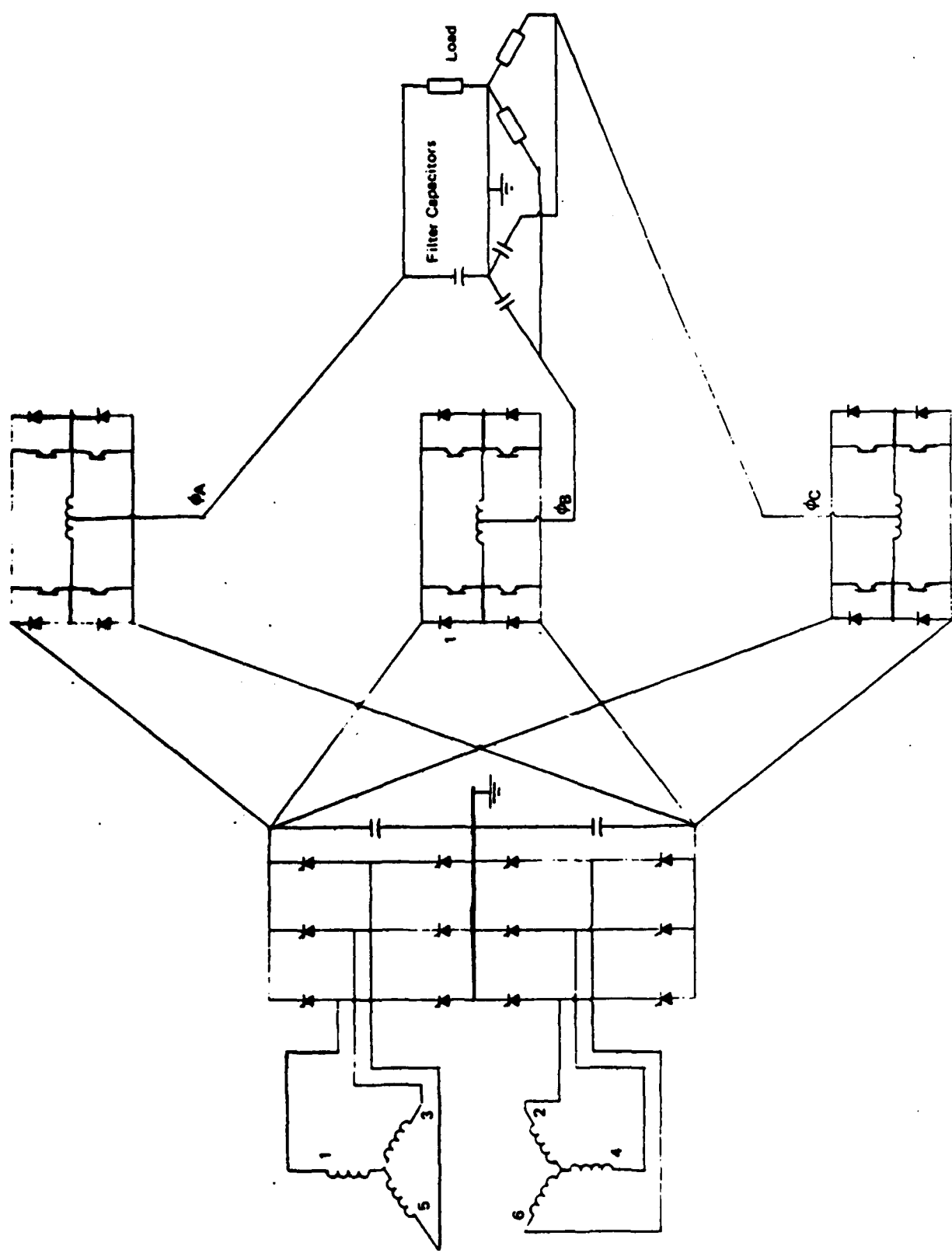


Figure 10. IPT-Inverter Power Circuit

- 2) The double frequency ripple current which flows through the DC link capacitor on the output of each 3 $\phi$  rectifier bridge in Figure 1 does not flow, except for unbalanced load conditions, in the DC link capacitors in Figure 10.

Figure 11 shows the switching sequence and voltages using standard triangle wave modulation.  $S_1$  and  $S_3$  cannot actually switch simultaneously but must have suitable delays to avoid the possibility of shoot-through currents which would occur if both transistors are allowed to conduct at once.

A complete switching sequence will be examined, first with current and voltage in phase and again with current and voltage out-of-phase.

Assume current and voltage are both positive (current flows into the load and the load voltage is positive with respect to ground). If switches  $S_1$  and  $S_2$  are both closed, current flows into the ends of the interphase transformer and out its center to the load. The output voltage is the + bus voltage neglecting switch and IPT losses. The interphase transformer forces equal sharing of current by  $S_1$  and  $S_2$  even though they have significantly different characteristics, since the ampere turns in the two windings must be equal except for excitation.

Next let  $S_2$  be opened and  $S_4$  closed. Equal currents must flow in both halves of the IPT so current must continue to flow into the right end of the transformer. Since  $S_2$  is open, current must flow up from the negative bus. With ideal switches, the pumpback diodes would not be required and this current would flow up through  $S_4$ . The practical requirement of delaying the closure of  $S_4$  until after  $S_2$  is open as well as the unipolar

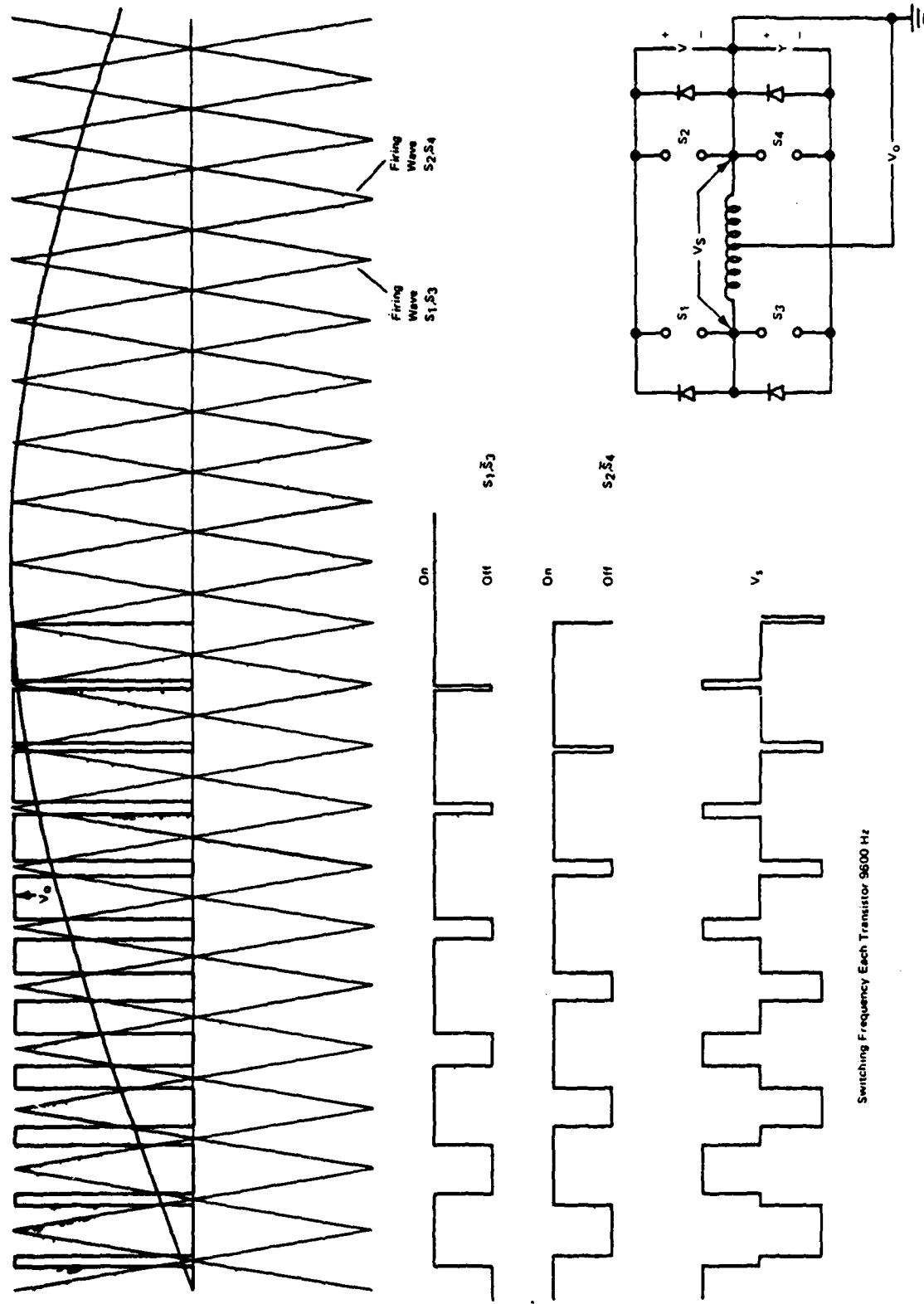


Figure 11. IPT Inverter-Switching Sequence

current flow of most semiconductor switches makes the diodes necessary thus the current path is up through diode 4. The IPT now spans the busses and its center tap is halfway between or at ground. When  $S_2$  is turned on again, the output returns to the + bus voltage. The cycle is completed by turning  $S_1$  off. Current flows through  $S_2$  and diode 3 and the output voltage is zero. Figure 12 shows the current paths for the four segments of the cycle. Next let the voltage remain positive but the current be negative as it would be with lagging load in the early part of a positive voltage half cycle.

The switching cycle is the same as before but the current paths are different. Referring to Figure 13 during interval one when  $S_1$  and  $S_2$  are closed, circuit flows up through their companion diodes. Output voltage is at the + bus as before.

When  $S_2$  opens and  $S_4$  closes, current flows down through  $S_4$  and continues through diode 1. The IPT again spans the voltage busses and the output voltage is zero.

Interval three is the same as one.

The cycle is completed with the opening of  $S_1$  and closure of  $S_3$ . Current flow is through  $S_3$  and diode 2. The IPT again forms a zero output voltage interval.

It has been shown that the IPT forces current sharing of even poorly matched switches. The second advantage of this circuit is in reducing the filtering required.

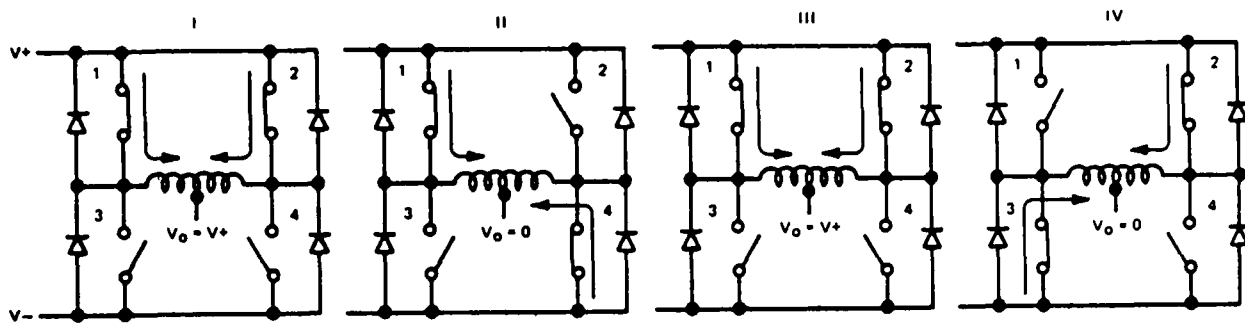


Figure 12. IPT Inverter - Current and Voltage Positive

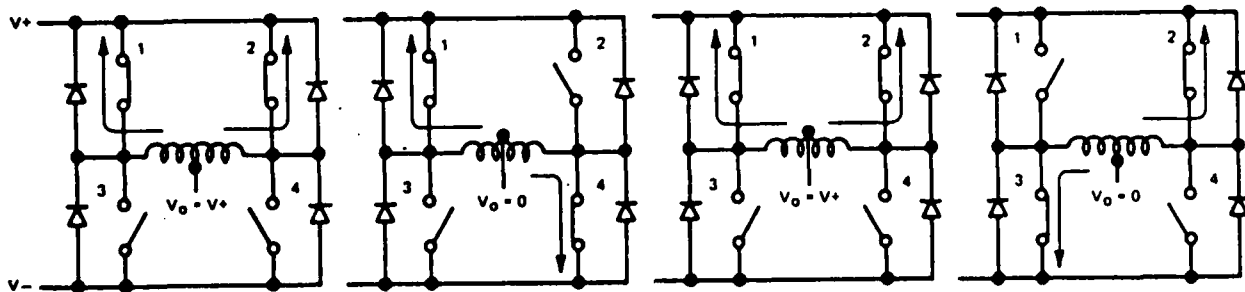


Figure 13. IPT Inverter - Current Negative Voltage Positive

The ripple voltage and currents of this circuit will be compared with a conventional inverter with the same switching frequency and then with a conventional inverter composed of two sets of switches, switching out of phase and summed through individual filter inductors rather than an IPT.

A simple switch pair generates zero average voltage by switching from the + to - bus and back at a constant rate. The ripple volt seconds are the bus voltage times the half period at the switching frequency. As the periods when the switches are connected to busses become unbalanced, the average voltage rises, and the ripple decreases as shown in Figure 14. Also shown in Figure 14 are the ripple volt-seconds for the IPT circuit. There is no ripple at zero output voltage as well as at full output. The peak ripple occurs at half maximum output and is one fourth the ripple volt-seconds of the single switch pair at zero output voltage.

There is a significant advantage in using the interphase transformer rather than paralleling switch pairs with out-of-phase switching patterns through simple inductors as shown in Figure 15. The ripple voltage at the load is identical to the IPT circuit but the ripple currents can be much different. The ripple current flowing to the load and filter capacitors are identical if the simple inductors for the two inductor circuits have twice the inductance of that of the IPT circuits. The ripple current flowing between the switch pairs can be independently controlled in the IPT circuit without changing the output impedance of the circuit by varying the IPT end to end inductance. In the two inductor circuits, the ripple current flowing between switch pairs can be reduced only by proportionately increasing the output impedance. Typically the IPT end to end inductance is twenty or more times the filter inductance so the current

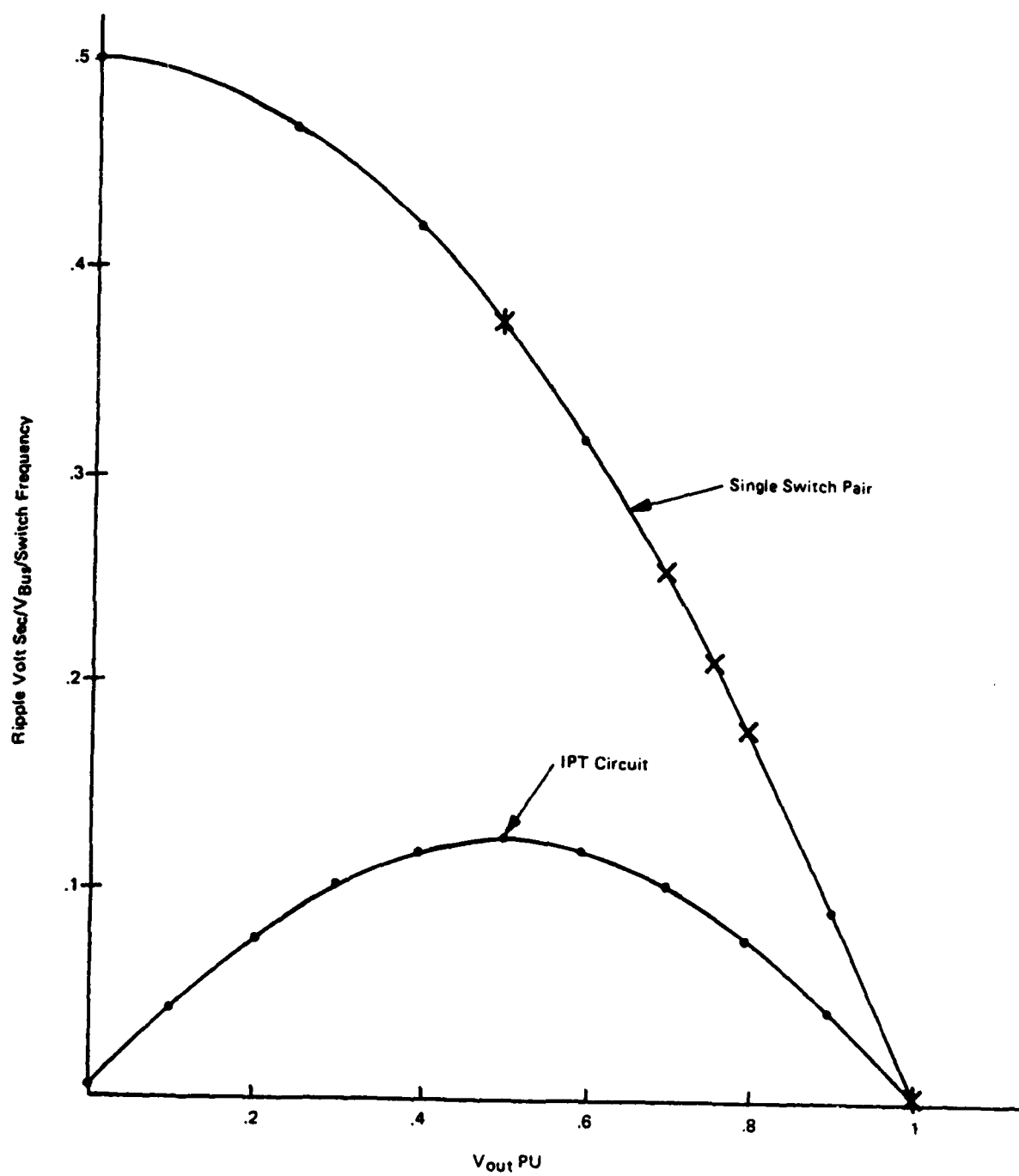
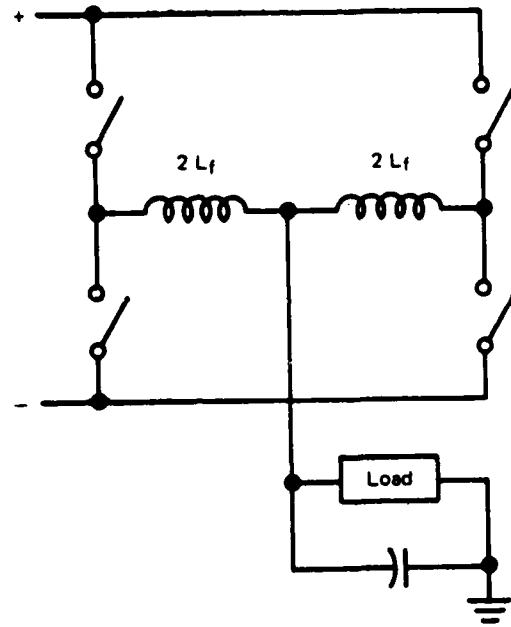
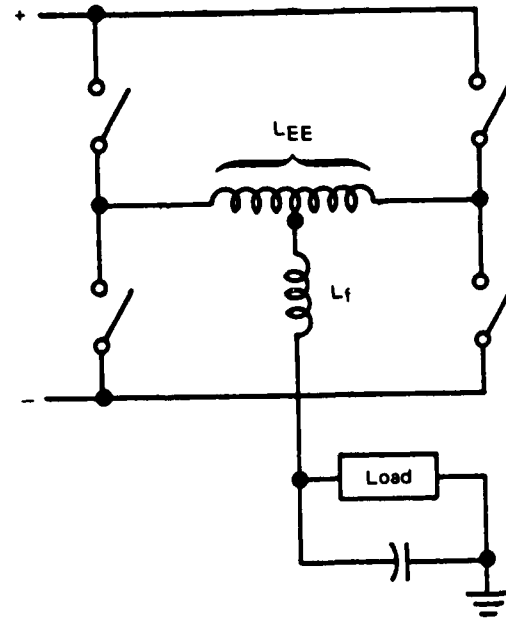


Figure 14. Ripple Volt - Sec vs Volts



Independent Inductors



IPT

Figure 15. Individual Inductors vs IPT

flowing between switch pairs is 1/5 or less than that of the two inductor circuit.

Minimizing ripple current results in some saving in  $I^2R$  loss but the major factor is reduction of the current which must be switched, which is the sum of load and peak ripple current. Unless the peak ripple current can be held to a small fraction of the load current, there is a large penalty in switching losses and load handling ability.

## Section V

### GENERATOR DESIGN

#### 1.0 DESIGN

The PWM converter circuit shown in Figure 1 required a nine phase generator to supply three 3-phase SCR bridges. This generator was the one which was designed originally. However, when it became apparent that the interphase transformer converter was a more attractive alternative than the 9 phase system, a change in the generator design from 9 to 6 phase output was necessary (see Section 4). This change only affected the stator windings, the rotor was not changed. The generator was designed to comply with the interface specifications. It was, after redesign, a six phase synchronous machine having a frequency of 1250 hz at base speed. The winding configuration was selected to be two isolated three phase windings to supply power to a positive DC link and a negative DC link in the converter. The generator layout is shown in Figure 16.

The speed range selected was 15,000 rpm to 30,000 rpm which is the specified speed range for the 60 KVA Advanced Development Program. The laboratory test model of the generator was configured to make maximum use of available tooling and test equipment, while maintaining the ability to easily convert to a production configuration. The rotor and stator are derived from the 60 KVA program and housed inside the stator frame of the F-18 generator. Although this frame is specifically designed for an integral generator/converter system, the basic design can be easily modified to permit separate mounting of the units in a production configuration, if desired.

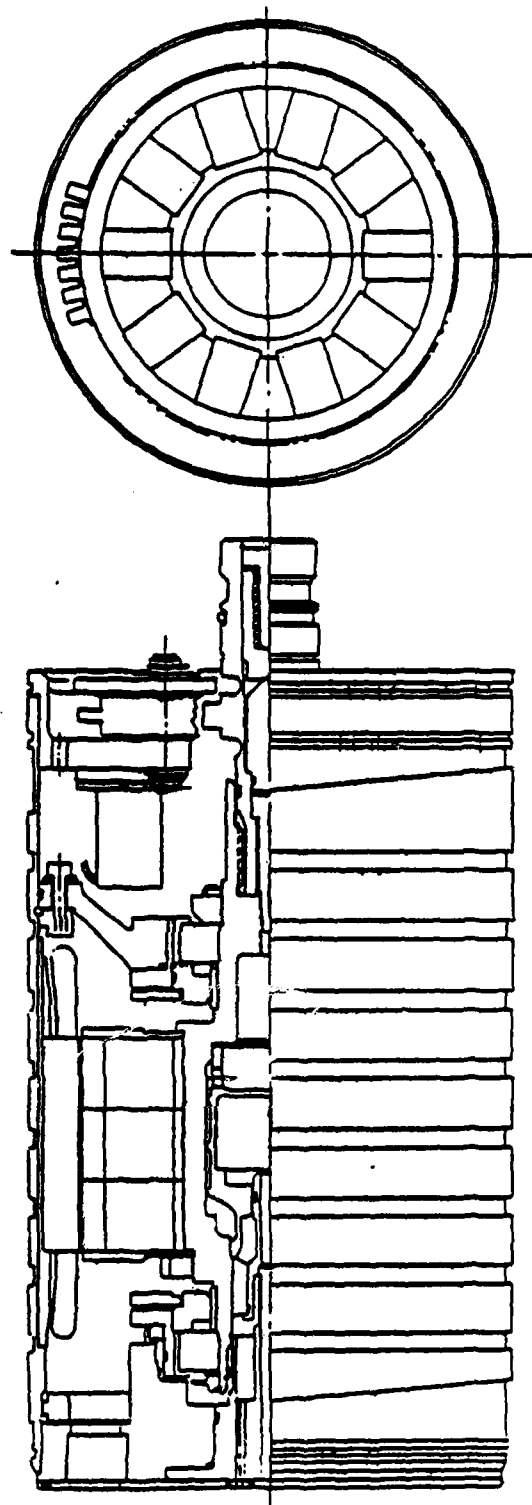


Figure 16. Generator Layout

The adapter required to test the generator is shown in Figure 17. The weight of the generator/adapter package is less than 75 pounds and exerts an overhung moment less than 500 inch pounds.

The oil flow schematic for the generator is shown in Figure 18. Cooling oil for the generator at base speed is approximately 4 gpm. The electromagnetic design, based on the use of the F-18 stator frame shown in Figure 19. has the following features:

1. The stator is a conventional aircraft design with 6 mil permendur lamination to minimize weight and increase efficiency by reducing core losses. The punching has 90 slots and is wound with 16 strands of No. 23 HML magnet wire. The total stack length required was 2.88 inches.
2. The rotor has 10 poles. The magnets are Samarium Cobalt having an energy product of 21 MGOe. (This is the highest level available in production quantities and expected to be competitively priced when production quantities will be required.)

The rotor hub is made from Inconel and the poles are made from low carbon magnetic steel. The magnets are contained by a bimetallic shrink ring having alternate magnetic and non-magnetic segments. The two bearings used are the MM9107 having an ABEC7 precision. Two seals are used at either end to maintain a dry rotor cavity. These seals are the circumferential type having spring loaded carbon riding on a film of oil.

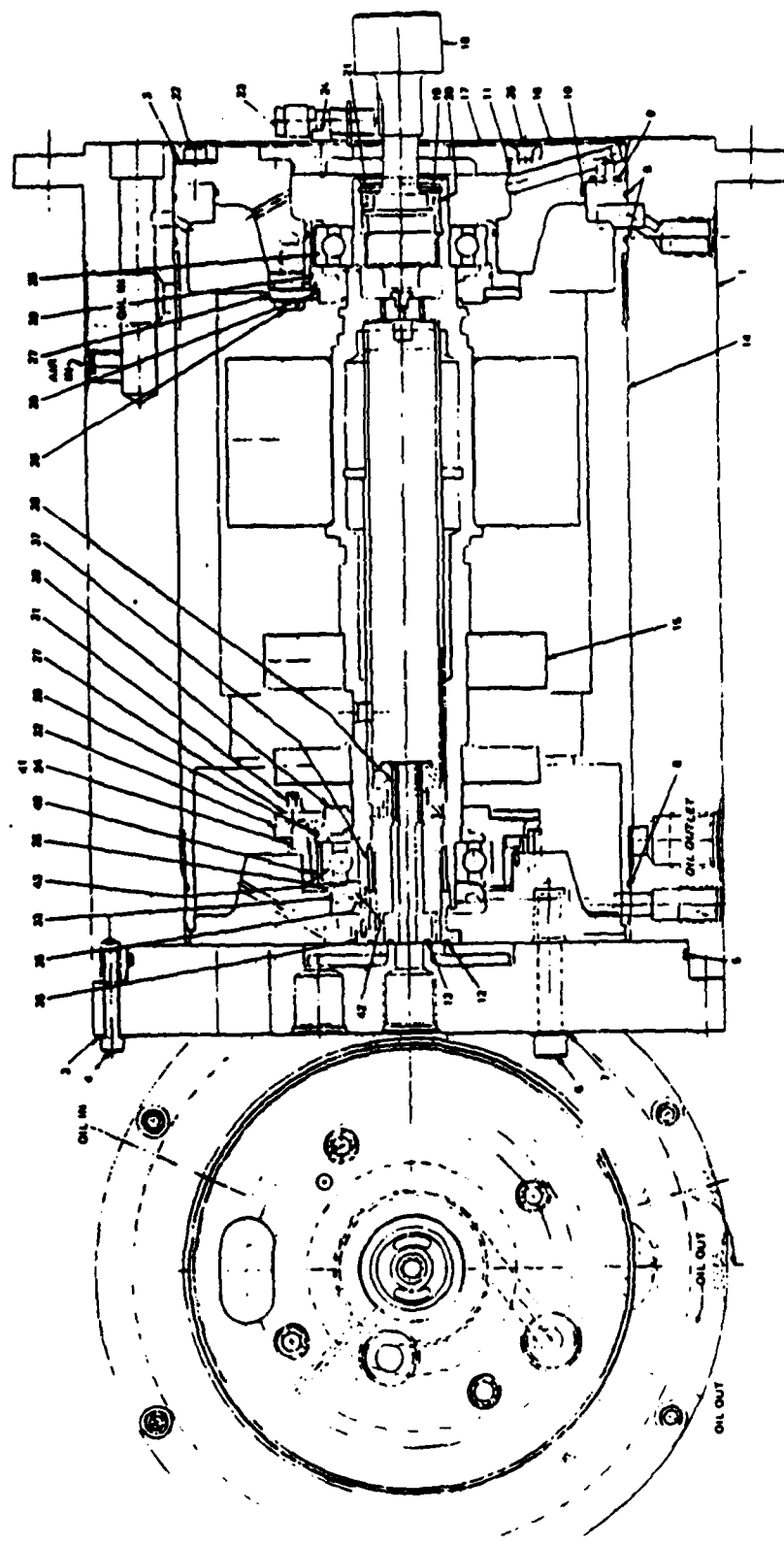


Figure 17. Generator Adapter

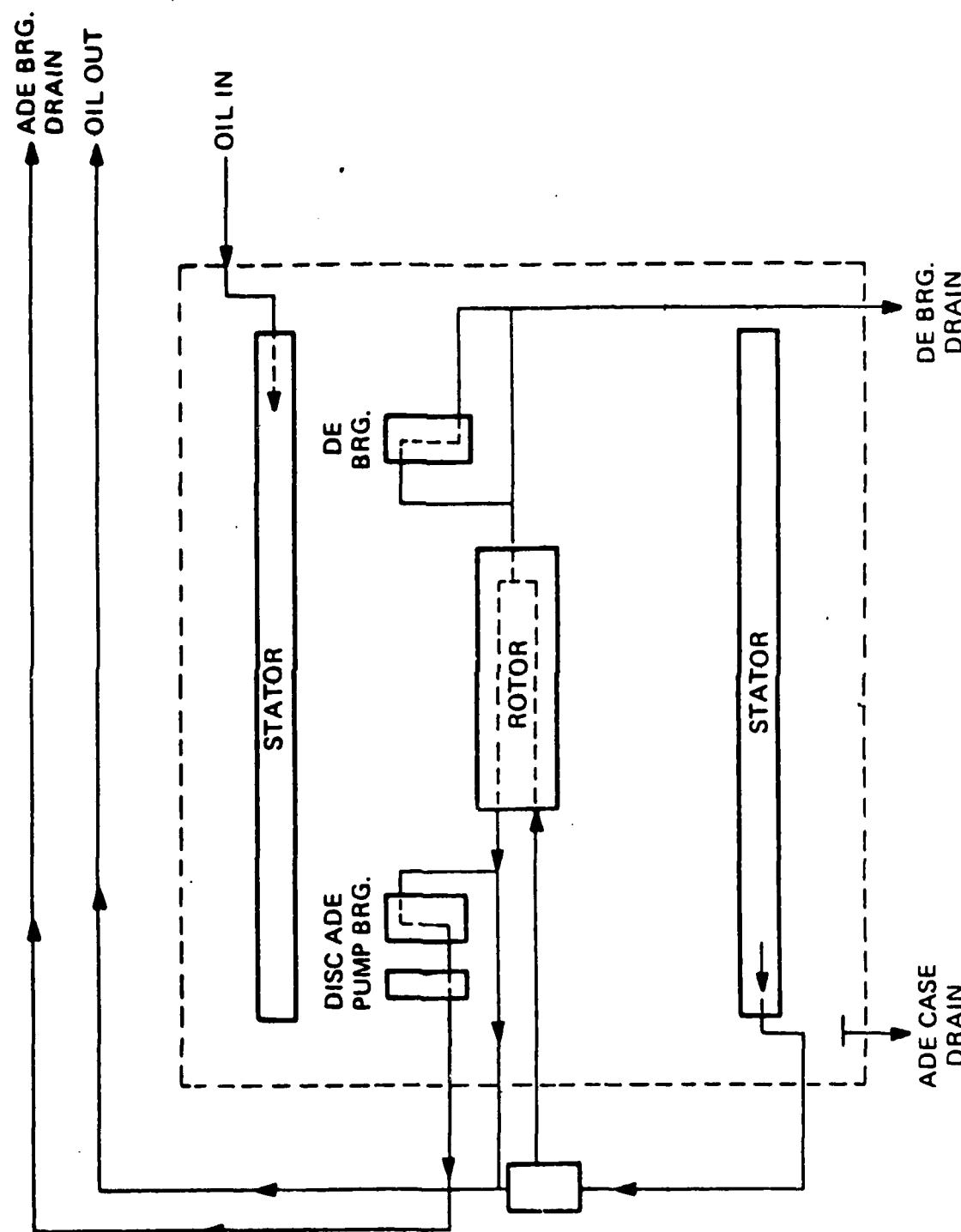


Figure 18. Generator Oil Flow Schematic

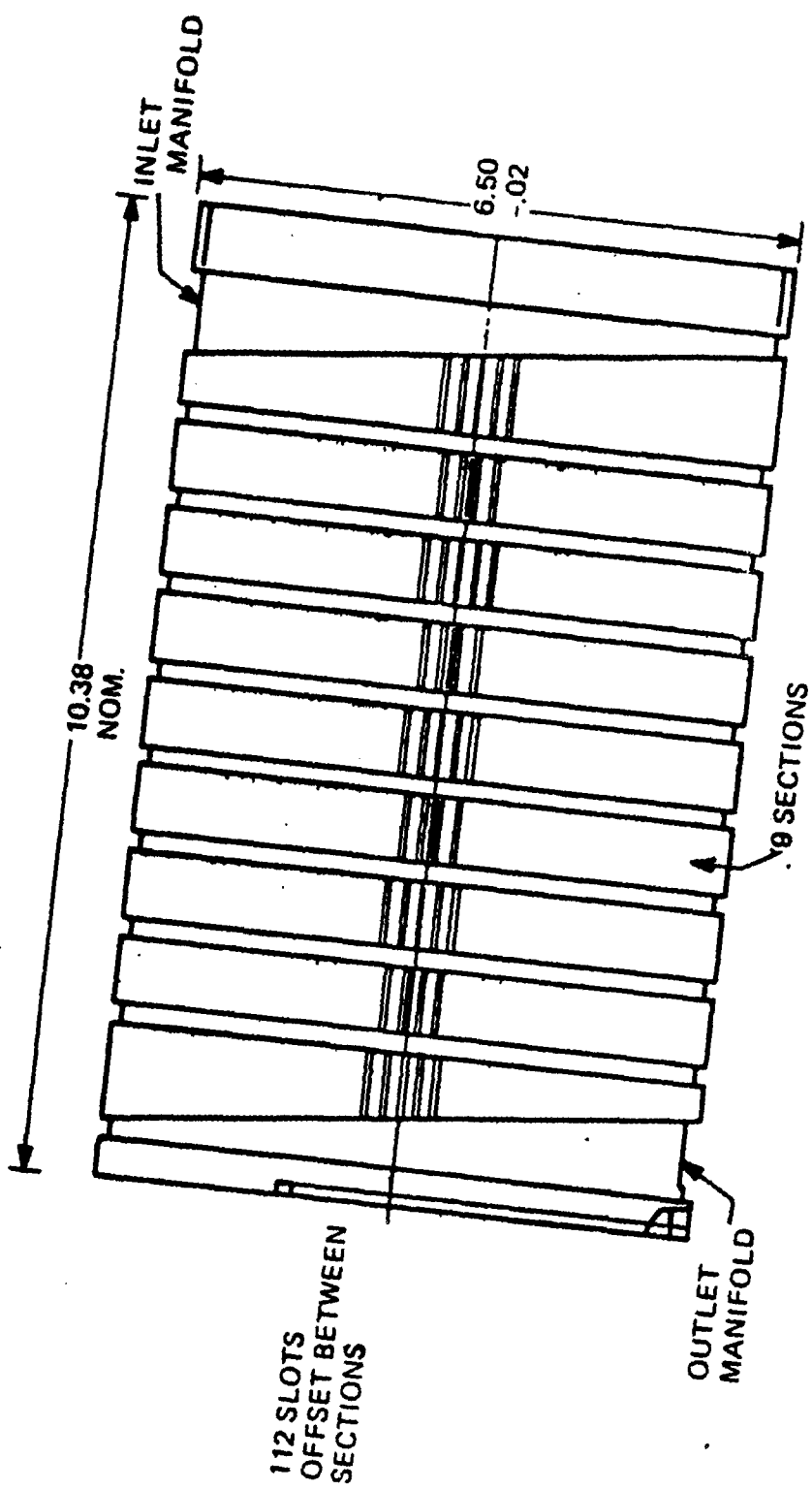


Figure 19. F-18 Stator Frame

## Appendix A

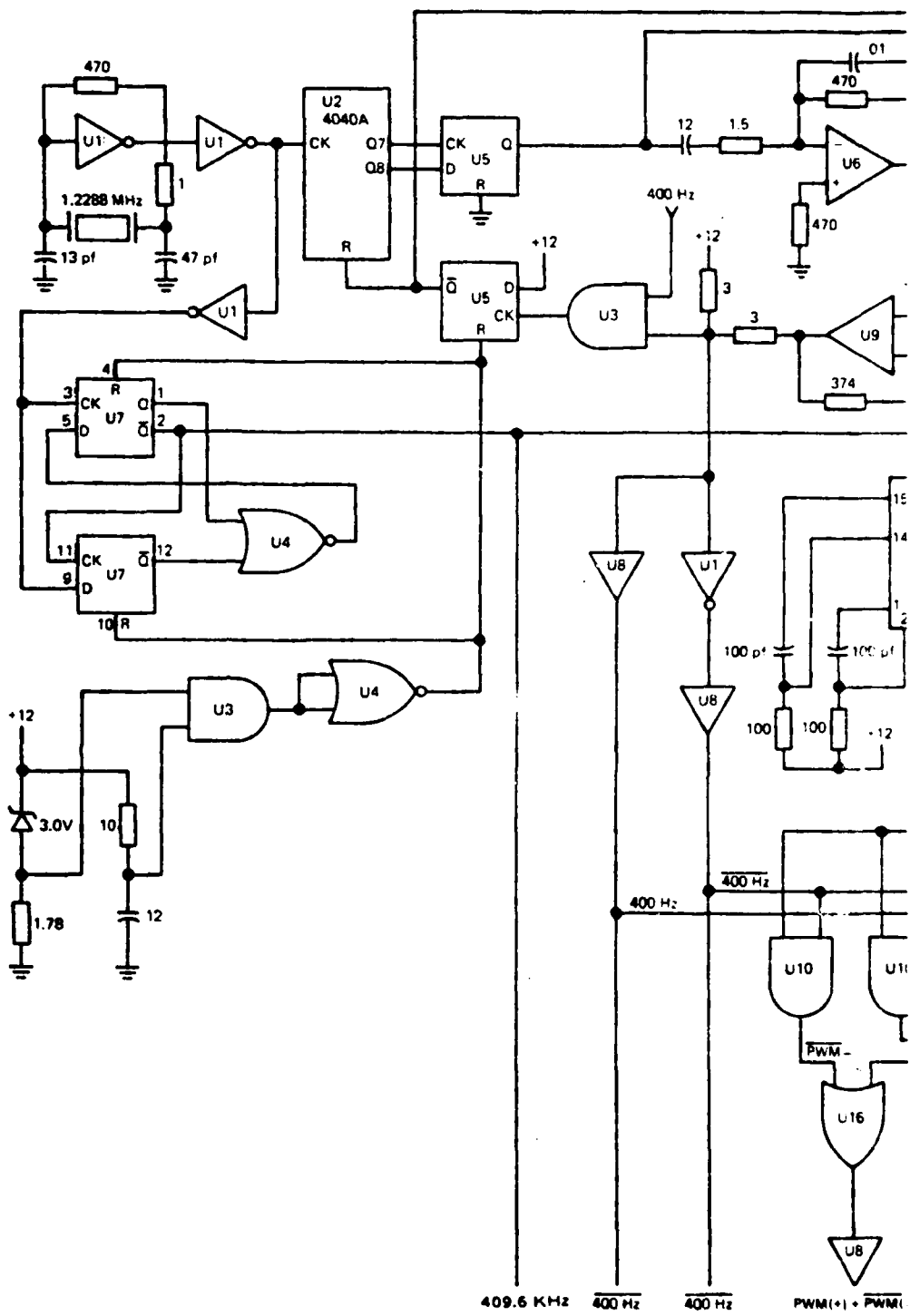
### ORIGINAL DESCRIPTION OF CMOS LOGIC

The entire CMOS control circuit is shown in Figure A-1. This current used CMOS logic to produce PWM signals for  $Q_1$  and  $Q_3$  (see Figure 3, Section III) and 400 Hz signals for  $Q_2$  and  $Q_4$ . The reference wave generator was a General Electric design which was originally used on the 60 KVA ADP and will not be discussed here.

A standard 1.2288 MHz crystal is used to generate a clock signal which is the input to a divide by three circuit and a 12 stage ripple carry binary counter/divider. The divide by three circuit (Figure A-2) produces 409.6 kHz, which is an input to the reference wave generator, which generates 400 Hz sinusoidal reference waves for each phase.

The counter outputs are 9600 Hz and 4800 Hz square waves, which are falling edge synchronized. These signals are inputs to a D type flip flop which changes the 4800 Hz signal to be using edge synchronized.

The capacitor in series with the output of the D flip-flop removes DC content from the 4800 Hz square wave, and the op-amp integrator creates a +6 volt to -6 volt triangular wave from the square wave. The output of this op-amp circuit is fed to a unity gain inverting amplifier, which inverts the 4800 Hz triangular wave. These two triangular waves are inputs to voltage comparators shown in Figure A-3. The other output to the comparator is the reference 400 Hz sinusoid, altered as necessary by DC feedback. The action



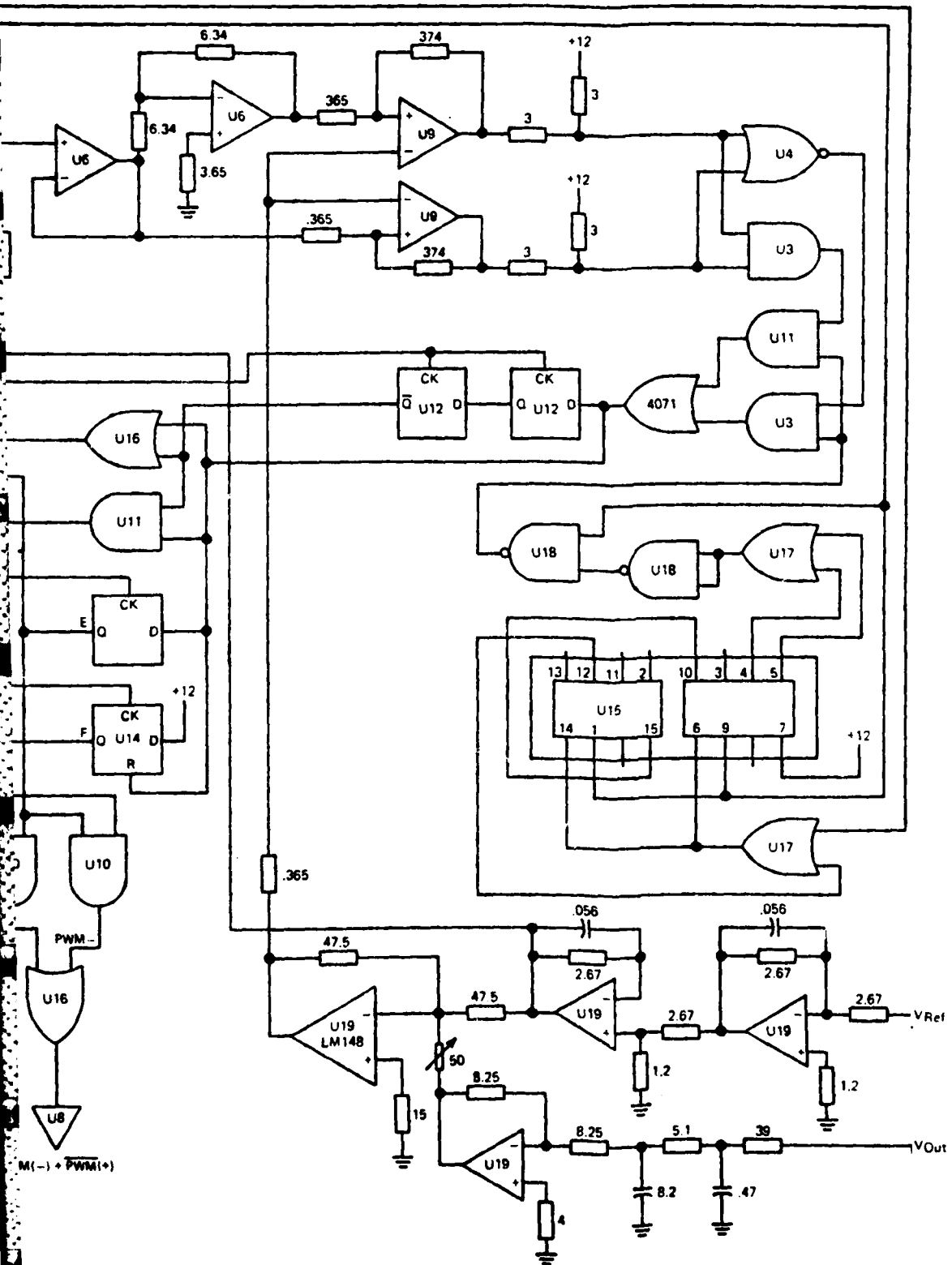


Figure A-1.  
PWM CMOS Logic - Single Phase Output

Timing Diagram for Divide-By-Three Counter

This circuit produces logic level (12 volt) falling edges corresponding to 409.6 KHz. This output goes to the reference wave generator to be used to generate 400 Hz sinusoidal reference waves for each phase.

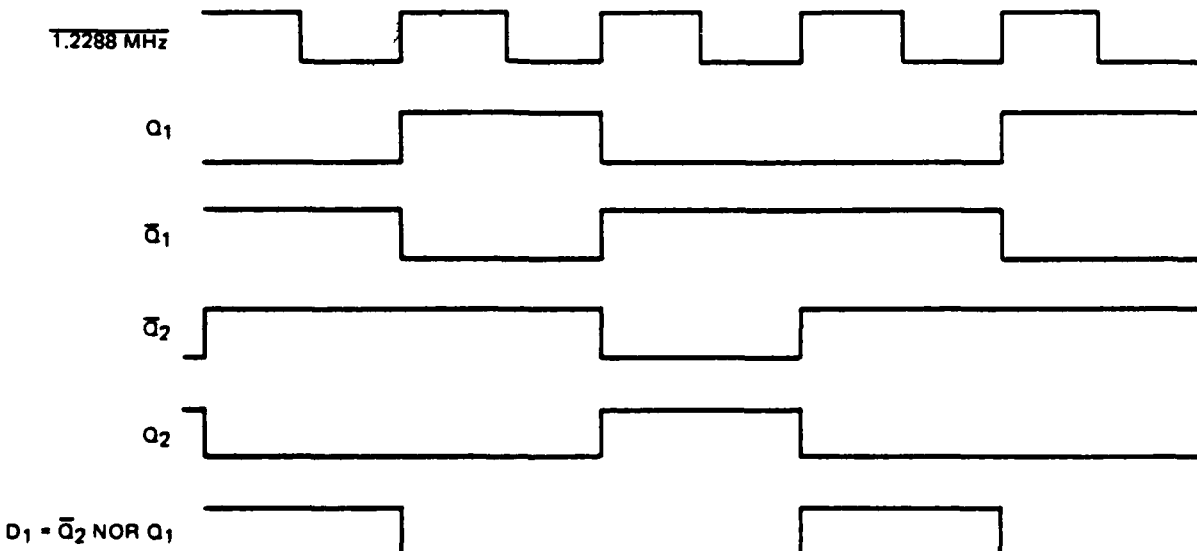
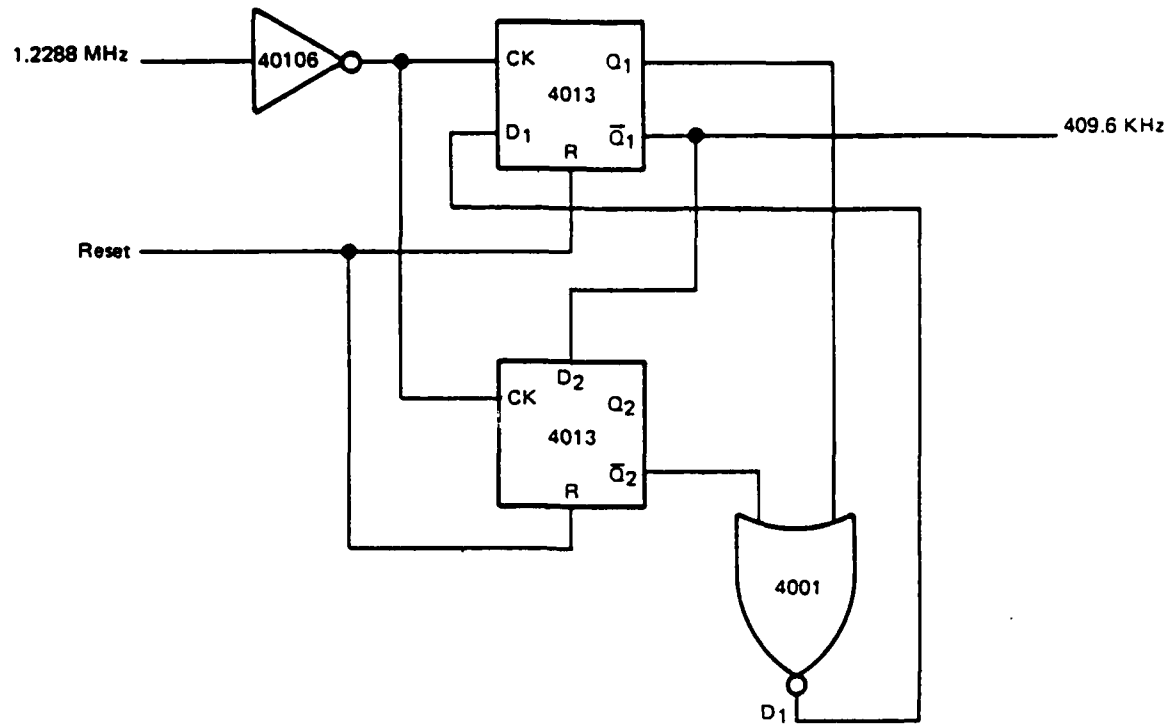


Figure A-2. Divide By Three Counter

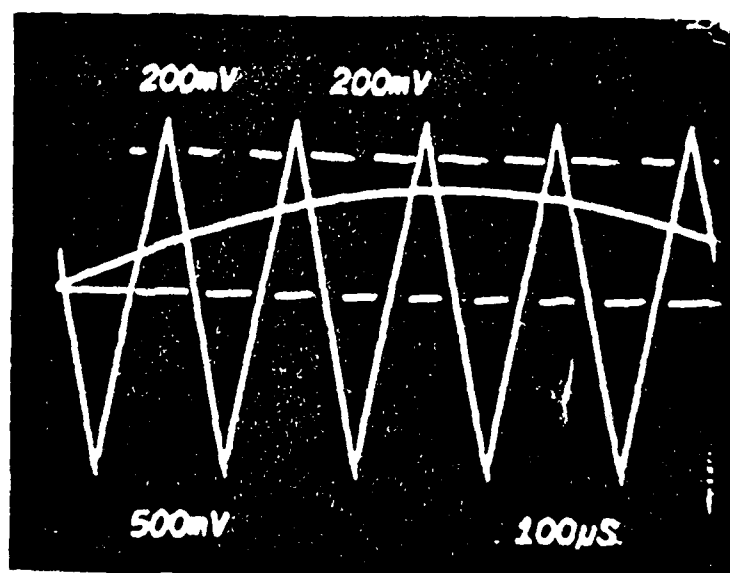
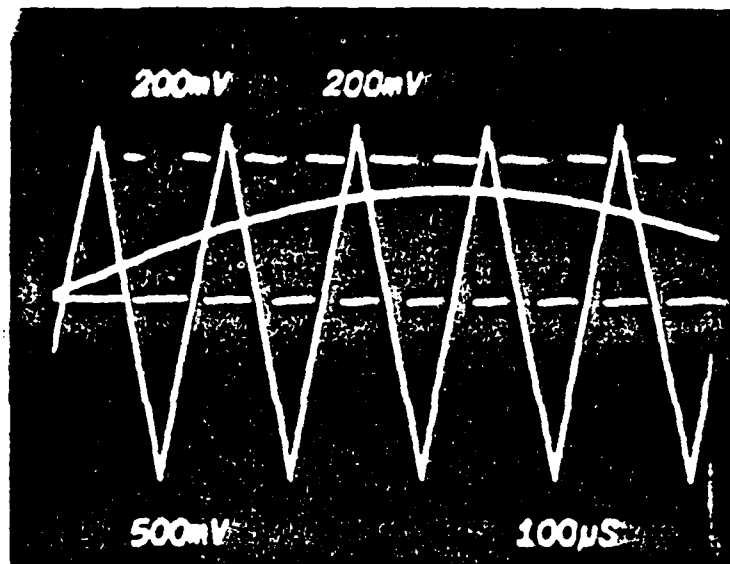
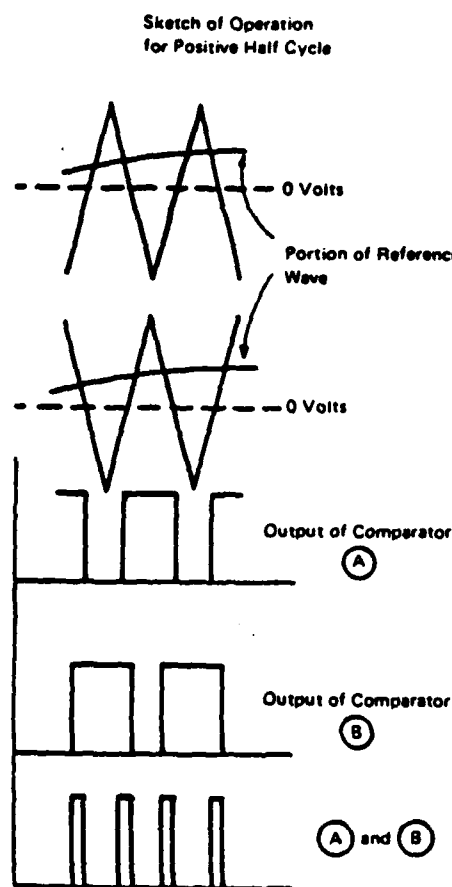
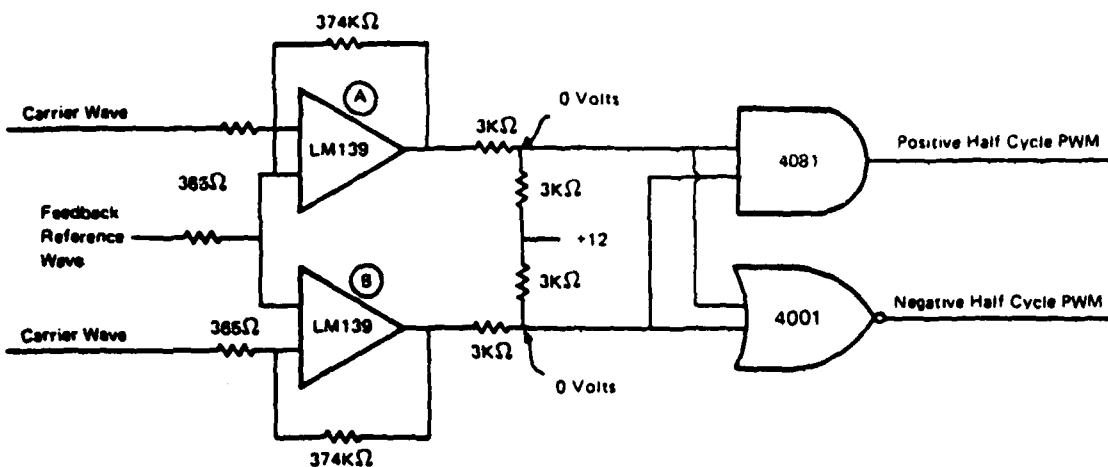


Figure A-3. PWM Voltage Comparators

of the LM139 is to produce a +12 volt signal when the triangular wave voltage is greater than the reference, and a -12 volt signal when the reference voltage is greater than the triangular wave voltage. The  $3\text{K}\Omega$  resistors connected to the outputs of the two LM139 voltage comparators act to make the LM139 outputs either 0 or +12 volts, rather than -12 or +12 volts. These comparator outputs are combined in an AND gate to produce the positive half cycle PWM, and in a NOR gate to produce negative half cycle PWM. This action is shown in Figure A-3. A LM139 was also used to produce the 400 Hz and 400 Hz square waves by detecting the zero crossings of the 400 Hz reference wave.

Spurious voltage spikes at the output of the LM139 voltage comparators which were generated when the 400 Hz reference wave passed through zero were eliminated by the circuit shown in Figure A-4. This circuit ensures that the logic level PWM signals remain at zero volts for a period of 7.5 electrical degrees (52.1  $\mu\text{s}$ ) centered around the 400 Hz reference wave zero crossing.

Figure A-5 shows the reference wave filter and DC content circuit. The reference wave filter is necessary to eliminate high frequency noise from the reference wave prior to it being used to create PWM and zero crossing signals. The DC content feedback circuit minimizes DC in the output waveform by altering the positive and negative half cycle PWM waveforms via the reference wave. Referring to Figure B-1, Appendix B, if the volt-second product of the positive half-cycle PWM is greater than the volt second of the negative half cycle PWM, there will be a DC voltage  $V_{BR}$  across the load. The DC feedback acts to increase the volt second product of the negative

half cycle PWM by subtracting a small DC voltage from the reference wave, effectively making the negative half cycle PWM pulses wider.

Figure A-6 shows the time delay/complement circuit which generated the  $\text{PWM}(+)$  or  $\overline{\text{PWM}}(-)$  and  $\text{PWM}(-)$  or  $\overline{\text{PWM}}(+)$  signals to turn the Darlintongs  $Q_1$  and  $Q_3$  on and off in a complimentary fashion. A time delay between pulses was necessary to prevent inadvertent shorting of the DC link voltage. This time delay had to be approximately 5  $\mu\text{s}$  to ensure that the Darlingtongs had time to turn off. The timing diagram for this circuit (Figure A-7) shows how the waveforms are generated. The waveforms E and F in Figure 8 are complements of each other, with time delays inserted. The AND and OR gates in Figure A-7 are used to generate the required signals which are then sent to the base drive circuits.

This completes a discussion of the original CMOS logic circuit. See Appendix B for a discussion of fourier analysis techniques applied to a pulse width modulated waveform.

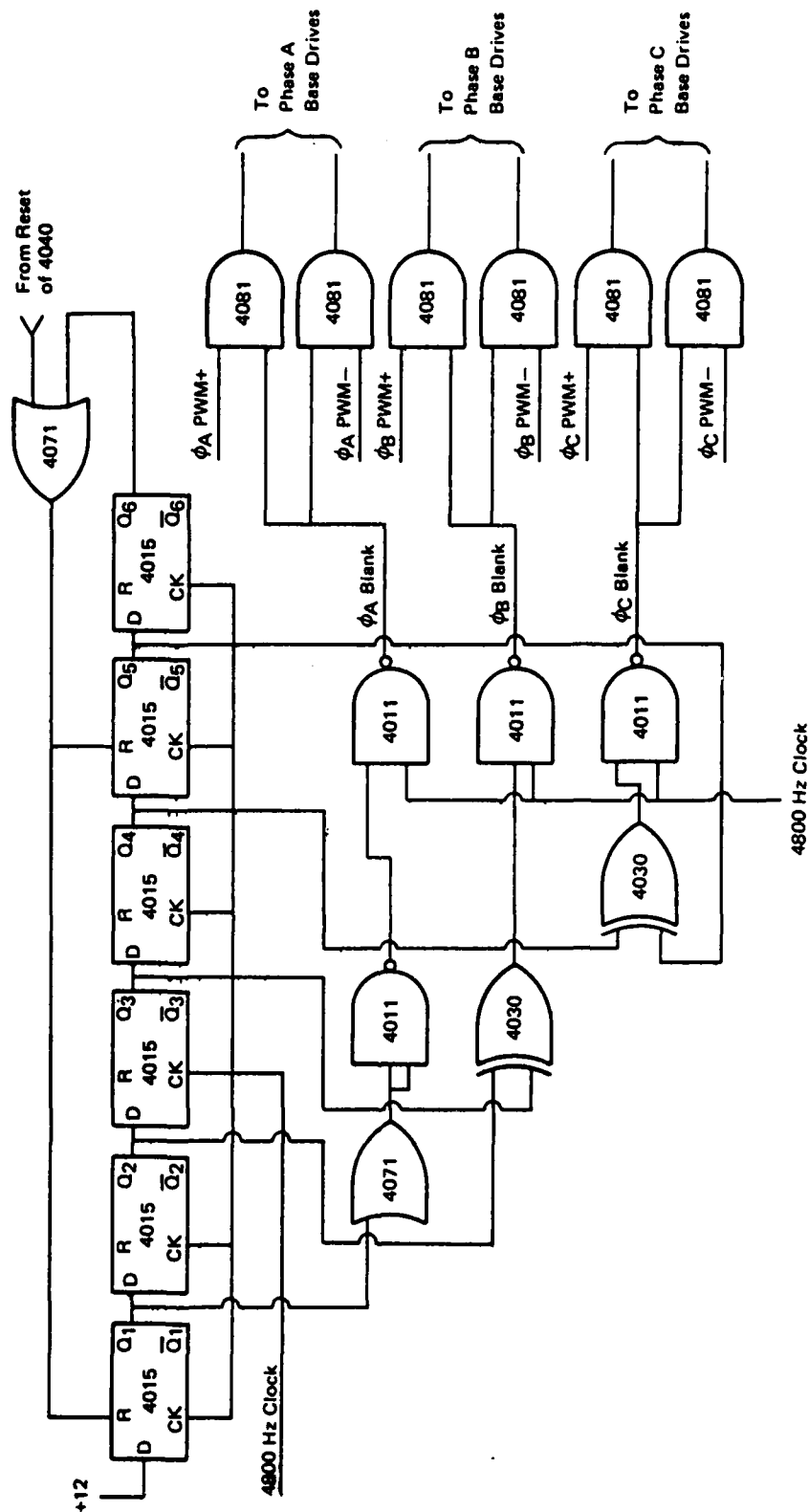
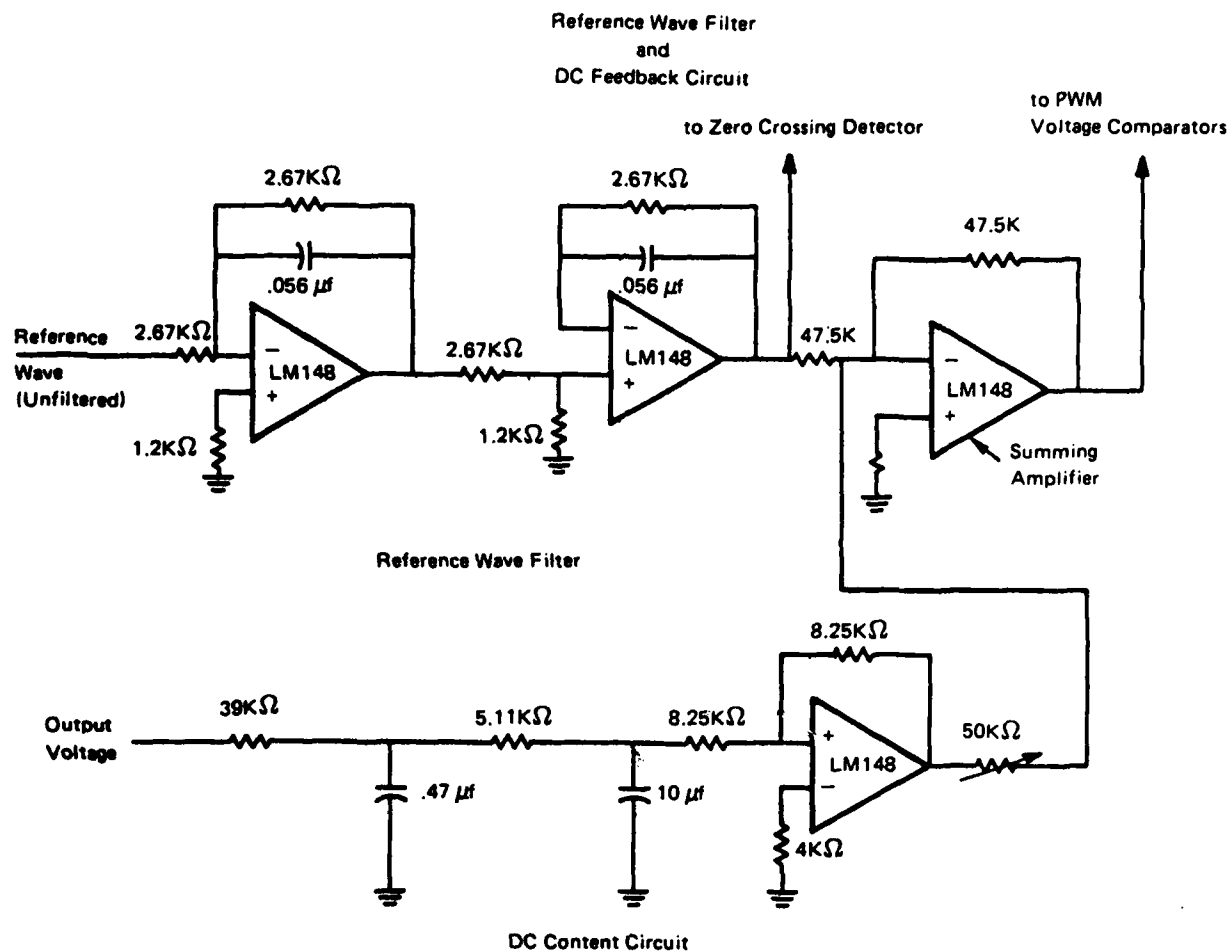


Figure A-4. Voltage Spike Blanking Circuit



**Figure A-5. Reference Wave Filter and DC Feedback**

The Reference Wave Filter is a double polefilter with a break frequency of 1064.4 Hz. This filter produces a "clean" reference for the zero crossing detector and the summing amplifier. The DC content circuit has two break frequencies, one at 8.68 Hz, the other at 3.11 Hz. This circuit produces a DC level proportional to the DC level in the output voltage. This DC level is summed with the "clean" reference wave and the output of the summing amplifier is used to produce PWM waveforms which are altered to eliminate dc in the output voltage.

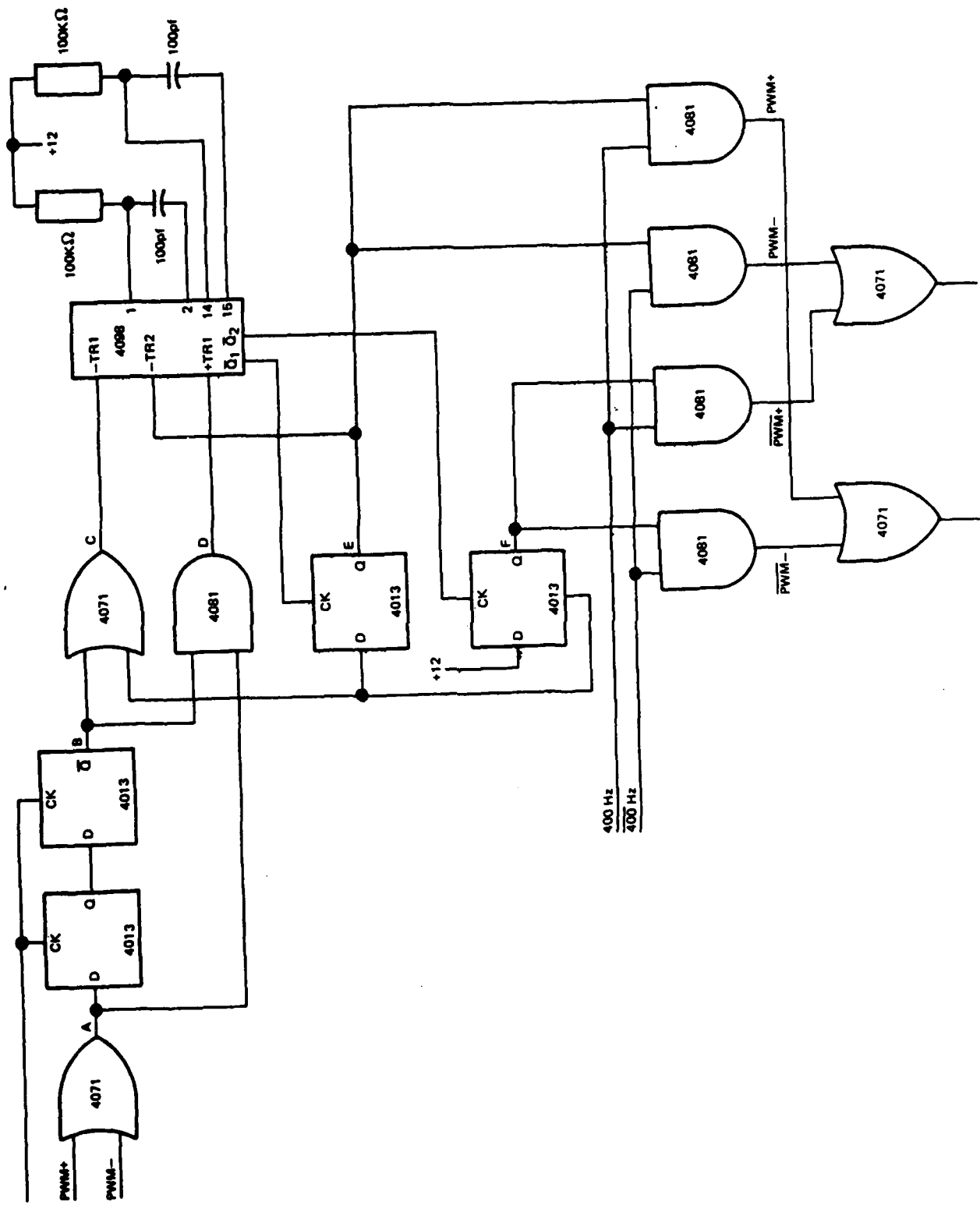


Figure A-6. Complement Circuit

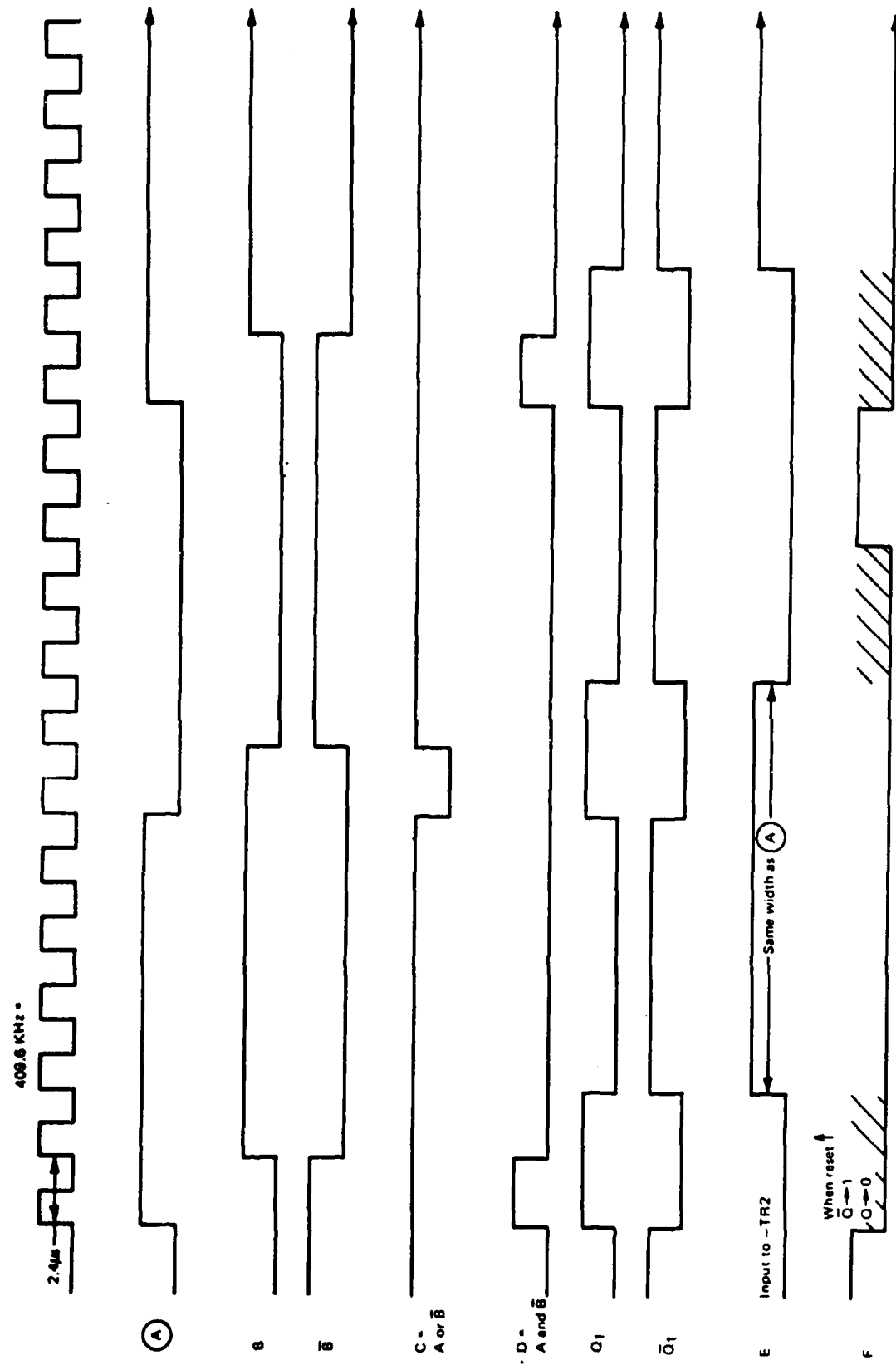


Figure A-7. Complement Circuit Timing Diagram

Appendix B  
FOURIER ANALYSIS OF PWM WAVEFORM

Harmonic analysis of the pulse width modulated output voltage waveform confirmed that the majority of the harmonic energy is located near the carrier wave frequency. The harmonic spectrum also varies as a function of the modulation ratio, defined in equation (1).

$$\text{Modulation Ratio } M = \frac{\text{Peak Voltage of Sinusoidal Reference}}{\text{Peak Voltage of Triangular Wave}} \quad (1)$$

Possible values of  $M$  range from 0 to  $\infty$ , with practical operation being confined to  $0 < M < 1.0$ . To determine the harmonic content of the PWM voltage waveform, the intersection points (or firing of angles) of the carrier wave and reference wave must be determined. This can be done by solving equation (2) for possible values of  $t$  (in  $\mu s$ ) or  $wt$  (in degrees of radians).

$$\begin{aligned} V_{\text{ref}} \sin wt &= Awt + B \\ wt &= 2\pi(400) \text{ rad/sec} \end{aligned} \quad (2)$$

The coefficients  $A$  and  $B$  are the slope and y intercept of the triangular wave carrier, referenced to a y-axis at the zero crossing of the reference wave.

Referencing Figure B-1, the PWM waveform is quarter and halfwave symmetric, so there is no DC component (ideally) and no cosine components in the Fourier series (again, ideally). In terms of a general Fourier series  $f(t)$ , equation (3),  $a_0 = 0$ , and

$$f(t) = \frac{1}{2} a_0 + a_1 \cos \omega t + a_2 \cos 2\omega t + \dots + b_1 \sin \omega t + b_2 \sin 2\omega t + \dots \quad (3)$$

$b_n = 0$ , leaving only the coefficients of the sine terms to be nonzero. In addition, since the PWM wave has half-wave symmetry, there will be no even harmonics in the output spectrum. Considering that  $f(t)$  in equation (4) is either  $V_{DC}$  or 0, if the firing angles are known, equation (4) becomes a trivial integral, whose solution is equation (5).

$$a_n = \frac{1}{\pi} \int_0^{2\pi} f(\omega t) \sin n\omega t d\omega t \quad (4)$$

$$a_N = \frac{4 V_D}{N\pi} \left[ \sum_{m=1}^6 \cos \theta_{2m-1} - \sum_{m=1}^6 \cos \theta_{2m} \right] \quad (5)$$

The variable  $N$  is the harmonic number, and the variable  $m$  designates the firing angle (see Table I).

Table II shows the harmonics of a PWM waveform with 24 firing angles per half cycle (9600 Hz carrier wave frequency). The results of this table show that no appreciable harmonics exist until the 21st harmonic (8400 Hz) is reached. The 23rd, 25th and 27th harmonics are also high, but after filtering they are reduced to below 1% of the fundamental.

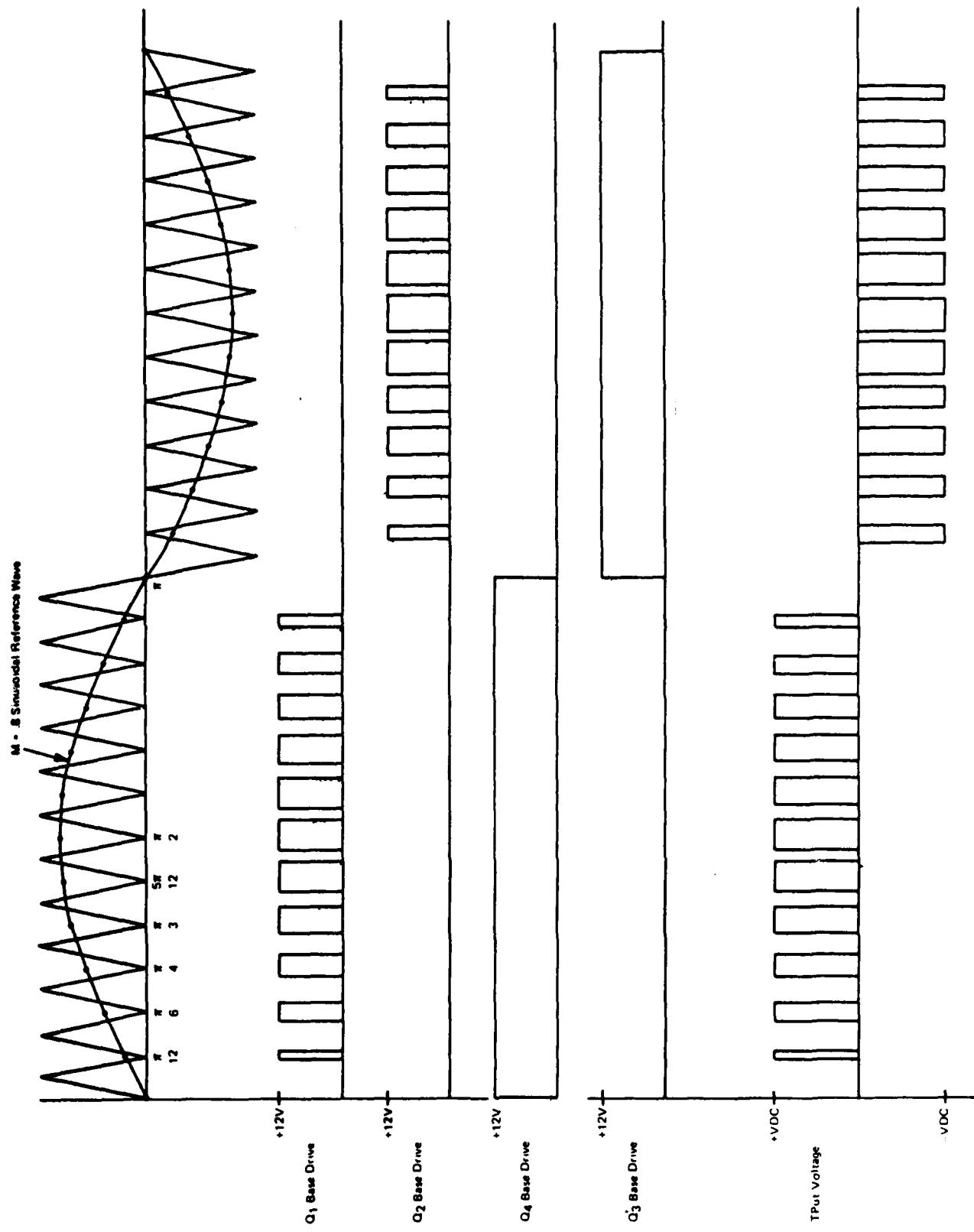


Figure B-1. PWM Waveform

TABLE I  
FIRING ANGLES FOR PWM WAVEFORM  
 $M = .85$

|               | $t$ ( $\mu s$ ) | $\omega t$ (deg) |
|---------------|-----------------|------------------|
| $\theta_1$    | 94.8            | 13.65            |
| $\theta_2$    | 117.7           | 16.95            |
| $\theta_3$    | 188.5           | 27.15            |
| $\theta_4$    | 233.3           | 33.60            |
| $\theta_5$    | 284.4           | 40.95            |
| $\theta_6$    | 346.9           | 49.95            |
| $\theta_7$    | 381.3           | 54.90            |
| $\theta_8$    | 457.3           | 65.85            |
| $\theta_9$    | 480.2           | 69.15            |
| $\theta_{10}$ | 565.6           | 81.45            |
| $\theta_{11}$ | 581.3           | 83.70            |
| $\theta_{12}$ | 625.0           | 90.0             |

TABLE II  
 HARMONIC CONTENT OF PWM WAVE  
 $M = .85$     $V_{DC} = 200.0V$

| N  | $V_N$  | $V_N/V_{DC}$ | $V_N/V_1$ | $20 \log V_N/V_1$ |
|----|--------|--------------|-----------|-------------------|
| 1  | 169.80 | .849         | 1.0       | 0                 |
| 3  | -.62   | 0            | 0         | $-\infty$         |
| 5  | .55    | 0            | 0         | $-\infty$         |
| 7  | -.66   | 0            | 0         | $-\infty$         |
| 9  | -.10   | 0            | 0         | $-\infty$         |
| 11 | -.41   | 0            | 0         | $-\infty$         |
| 13 | -.47   | 0            | 0         | $-\infty$         |
| 15 | .61    | 0            | 0         | $-\infty$         |
| 17 | -.64   | 0            | 0         | $-\infty$         |
| 19 | -2.90  | .014         | .0165     | -82.1             |
| 21 | -32.81 | .164         | .1937     | -32.82            |
| 23 | -55.10 | .2755        | .3245     | -22.51            |
| 25 | 59.41  | .2970        | .3498     | -21.00            |
| 27 | 30.83  | .1541        | .1815     | -34.13            |
| 29 | 2.34   | .0117        | .0138     | -85.66            |
| 31 | 0.06   | 0            | 0         | $-\infty$         |

## Appendix C

### DARLINGTON PARALLELING STUDY

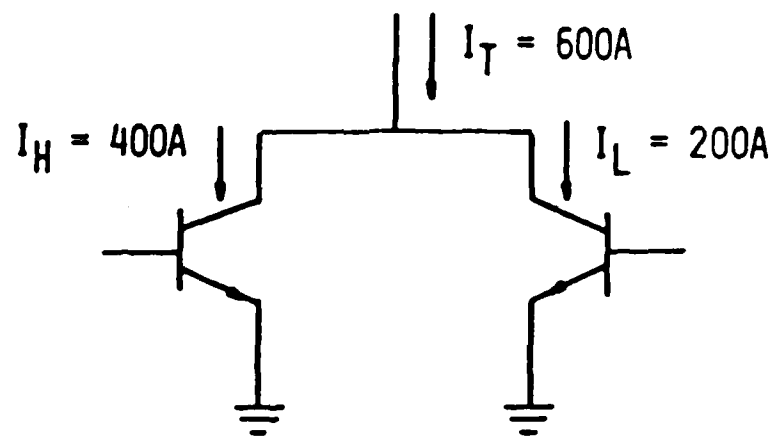
The Solid State Applications Operation (SSAO) of General Electric performed a study of the problems involved in paralleling ZJ504 Darlington transistors, since two or three Darlintongs in parallel would be necessary to support fault conditions based on a 40 KVA system rating, using the original configuration. The peak fault current for a 3 per unit (p.u.) fault through each leg of the bridge would be approximately 600 Amperes, far exceeding the rating of a single device. The ZJ504 has the capability of supporting 200 Amps continually, and 400 Amps for 100  $\mu$ s. When two devices are placed in parallel, the ability which they show to share current can be shown by the coefficient M, derived in Figure C-1. When M is unity, each device would conduct half the total current flowing in one leg of the inverter bridge.

Assuming an M of 1.1 and a 3 p.u. fault current means that the peak current flowing through the device carrying 52% of the current is 312 Amps. This current is below the 400 Amp/100  $\mu$ s criteria outlined above, but there is a 700  $\mu$ s period in each cycle where currents in each device are above 200 Amps. It is this period which was of concern as to whether the device would handle the current requirements.

The manner in which SSAO tested for parallel operation was to use the circuits shown in Figures C-2 and C-3 to switch the devices at approximately 10 KHZ to evaluate both steady state and dynamic matching. The results of these tests were that 1) Dynamic matching did not appear to be as severe a problem as

originally thought and 2) 22.76 Kw at 280 volts DC was successfully switched.

However, during this testing, four devices were destroyed, each failing due to an overvoltage condition. The first device to fail (Serial Number 194) was exposed to an overvoltage condition which stressed SN 199 also. Then, SN 199 failed when a snubber diode failed, overstressing SN 197. Serial Number 197 failed during a test where it was exposed to >500 volts, overstressing SN 255, which then failed during increased power testing.



$$\text{FRACTIONAL MATCH} = \frac{I_H}{I_L} = M$$

THEN,

$$I_H = \frac{I_T}{\left(1 + \frac{1}{M}\right)}$$

Figure C-1. Current Sharing and Matching Definition

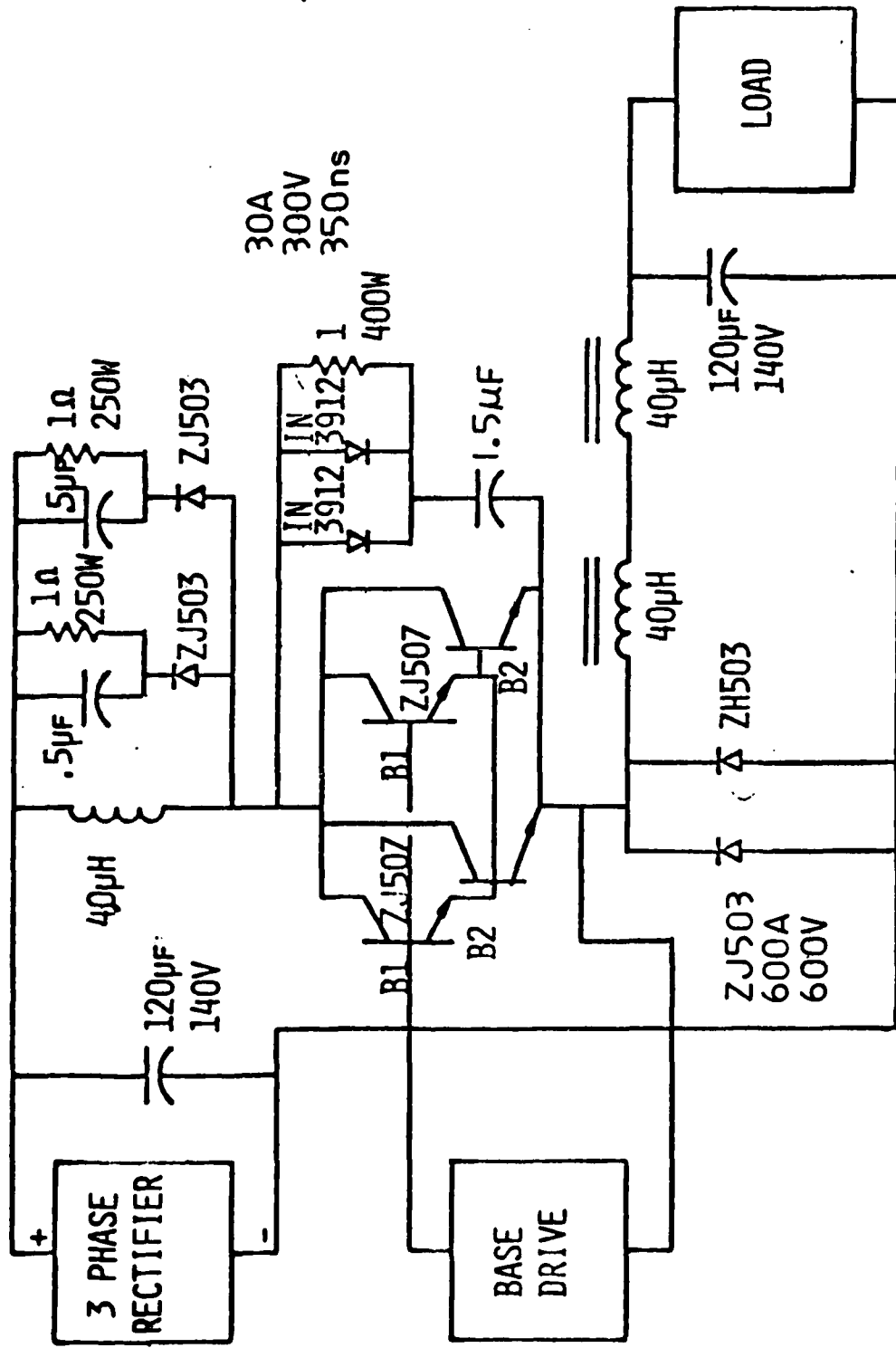


Figure C-2. Switching/Paralleling Circuit

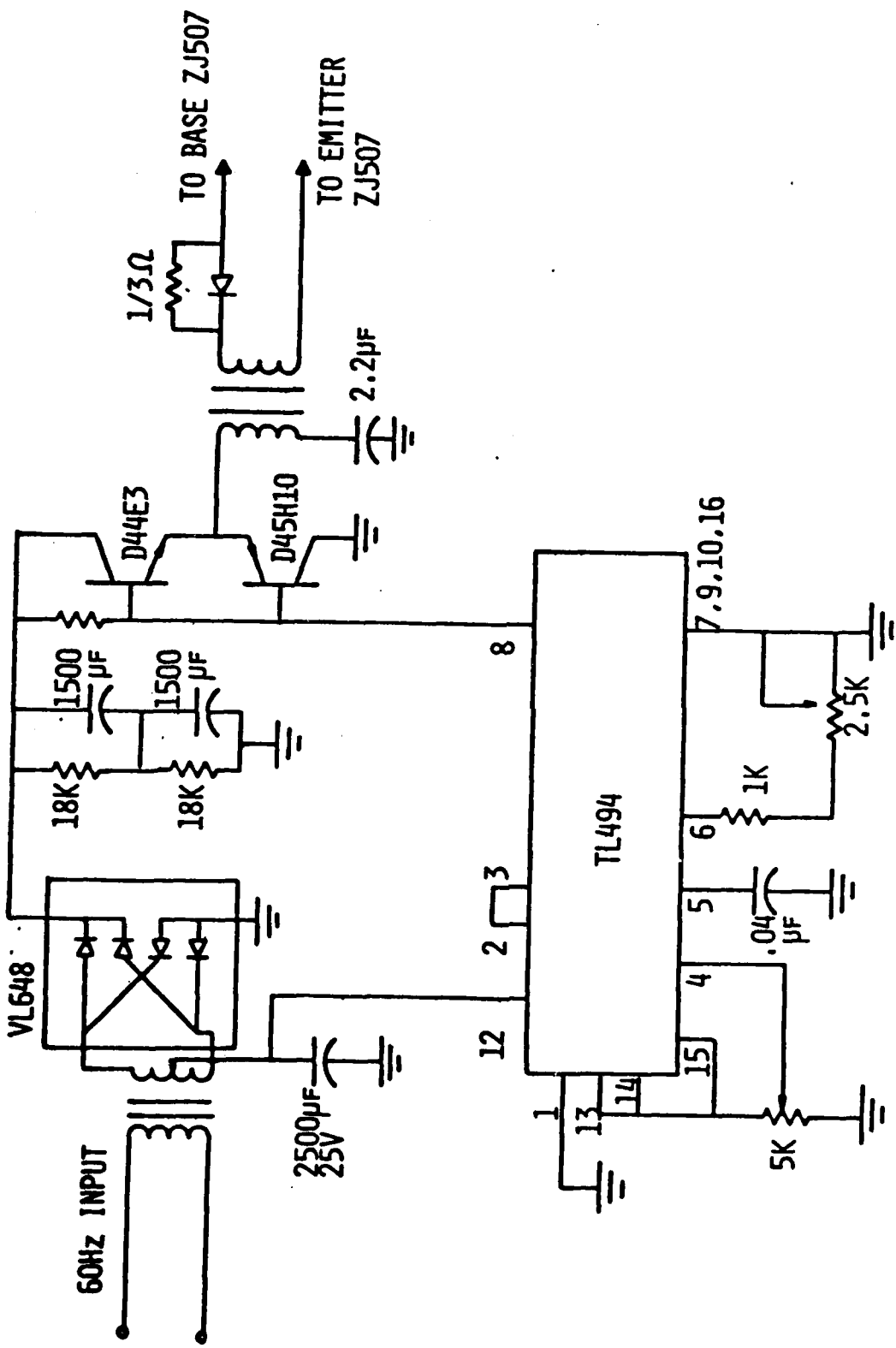


Figure C-3. Base Drive Used by Solid State Applications Organization, General Electric Company

**Reference**

1. "Supplying the Analysis of Harmonic Content in Complex Inverter Switching Waveforms," R.H. Lee, Proceedings of Powercon 8, 1981

END

FILMED

20

DIE